Mon. Not. R. Astron. Soc. **000**, 000–000 (0000) Printed 20 May 2009 (MN LATEX style file v2.2)

Energy ejection in the collapse of a cold spherical self-gravitating cloud

M. Joyce[1], B. Marcos[2,3,4] and F. Sylos Labini[2,3]
[1] *Laboratoire de Physique Nucléaire et de Hautes Energies, UMR 7585, Université Pierre et Marie Curie — Paris 6, 75252 Paris Cedex 05, France*
[2] *"E. Fermi" Center, Via Panisperna 89 A, Compendio del Viminale, I-00184 Rome, Italy*
[3] *ISC-CNR, Via dei Taurini 19, I-00185 Rome, Italy*
[4] *Laboratoire J.-A. Dieudonné, UMR 6621, Université de Nice — Sophia Antipolis, Parc Valrose 06108 Nice Cedex 02, France*

20 May 2009

ABSTRACT
When an open system of classical point particles interacting by Newtonian gravity collapses and relaxes violently, an arbitrary amount of energy may in principle be carried away by particles which escape to infinity. We investigate here, using numerical simulations, how this released energy and other related quantities (notably the binding energy and size of the virialized structure) depends on the initial conditions, for the one parameter family of starting configurations given by randomly distributing N cold particles in a spherical volume. Previous studies have established that the minimal size reached by the system scales approximately as $N^{-1/3}$, a behaviour which follows trivially when the growth of perturbations (which regularize the singularity of the cold collapse in the $N \to \infty$ limit) are assumed to be unaffected by the boundaries. Our study shows that the energy ejected grows approximately in proportion to $N^{1/3}$, while the fraction of the initial mass ejected grows only very slowly with N, approximately logarithmically, in the range of N simulated. We examine in detail the mechanism of this mass and energy ejection, showing explicitly that it arises from the interplay of the growth of perturbations with the finite size of the system. A net lag of particles compared to their uniform spherical collapse trajectories develops first at the boundaries and then propagates into the volume during the collapse. Particles in the outer shells are then ejected as they scatter through the time dependent potential of an already re-expanding central core. Using modified initial configurations we explore the importance of fluctuations at different scales, and discreteness (i.e. non-Vlasov) effects in the dynamics.

Key words: Virialization; spherical collapse; N-body simulations

1 INTRODUCTION

That isolated systems of initially cold self-gravitating particles collapse and relax violently to produce virialized quasi-equilibrium structures has been known for many decades — essentially since numerical simulation of such systems began (see, e.g., Hénon (1964)). In cosmology it has emerged in the last decade or so, through large numerical simulations, that a good approximate description of the structures formed can be given in terms of "halos", which are similar quasi-equilibrium structures formed from collapse of matter in finite regions, containing initially cold (dark matter) particles (for a review, see e.g. Cooray & Sheth (2002)). Analytical understanding of the strongly non-linear physics involved in the formation of these quasi–equilibrium states is, despite the importance of the problem and many attempts to solve it, extremely limited. For example, while the simple density profiles which result from a class of uniform initial conditions have been known since early numerical studies (see, e.g., van Albada (1982) and references therein), there is still no theory which can clearly explain them. Likewise, in cosmology, numerical evidence for the "universality" of certain simple halos profiles (different to those obtained from quasi-uniform cold collapse) has been produced (Navarro et al. (1996, 1997)), but understanding of the physical reason for the ubiquity of these profiles is still lacking.

In attempts to gain greater insight into the physics leading to such virialized states, with the goal notably of understanding the dependence of their properties on initial conditions, one angle of approach, which is the one adopted here, is to study in detail the evolution from some limited class of initial conditions. We focus here on what appears to us a neglected, and potentially important, aspect in the study of

collapse and virialization of open self-gravitating systems: in the phase of (violent) relaxation such systems may, in general, eject a fraction f^p of their mass which carry away a finite amount of energy K^p as kinetic energy, i.e., some of the particles come out of the collapse with positive energy and may escape to infinity. The binding energy and characteristic size of the virialized state, in particular, are directly related to these ejected quantities. Indeed, using (1) total energy and mass conservation, (2) the virial condition for the bound particles, and (3) neglecting the potential energy between the bound and escaping particles, and that of the escaping particles themselves, it follows that

$$W^n = 2(E_0 - K^p) \tag{1}$$

where W^n is the (negative) potential energy of the bound particles, and E_0 is the total initial energy. While for $E_0 > 0$ some energy must be ejected, for $E_0 < 0$ energy may, or may not, be ejected. In principle there is no upper bound on this ejected energy (as there is no lower bound on the gravitational potential). Indeed it is known that a self-gravitating system of point particles is intrinsically unstable towards the ejection of an infinite amount of energy — the so-called "gravo-thermal catastrophe" (Lynden-Bell & Wood 1968; Binney & Tremaine 1994). This instability is understood, however, to be relevant in practice only on time scales which diverge with particle number N. The term "violent relaxation", on the other hand, refers precisely to a physical relaxation process which takes places on much shorter scales, involve purely mean field (i.e. "collisionless") physics (Lynden-Bell 1967). In the study we present in this paper we will see that the energy ejected on these shorter time scales, during violent relaxation, appears to be unbounded above for the class of initial conditions we study. Further we will investigate whether the ejection we observe in our simulations can be fully understood as a mean field phenomenon.

The central considerations in this article — energy ejection and the validity of the mean field limit in cold collapse — are of relevance in theoretical attempts to understand violent relaxation. For example, the original theory proposed by Lynden-Bell (1967) to predict the properties of virialized states made both the assumption that these states have the same energy and mass as the initial conditions, and that the dynamics is purely mean field (i.e. governed by the Vlasov-Poisson equations). Although this theory is believed to be inadequate[1] — and in any case it may not be applicable to the particular set of cold initial conditions we study — such assumptions are usually made in theoretical approaches to understanding these states. It is thus important to understand the extent to which they are valid. Interestingly we find in our simulations that the *shape* of the density profiles of the relaxed systems appear to be very robust, i.e., independent of the initial conditions, despite the fact that their global macroscopic parameters, notably their mass and energy, vary with N.

In this article we address these questions primarily using the very restricted set of initial conditions given by distributing N particles randomly in a spherical volume, and ascribing zero velocity, i.e., a sphere of cold matter with Poissonian density fluctuations. The simplicity of these initial conditions is that they are characterized by the single parameter N. On the other hand, they present an intrinsic numerical complexity: while the problem is well defined for any finite N, it tends formally, as $N \to \infty$, to the exactly uniform spherical collapse which leads to a density singularity at a finite time. This makes it expensive to integrate numerically for increasing N. Indeed for this reason many authors have excluded it from numerical studies, focusing instead on spherical models with non-trivial inhomogeneous distributions (e.g. radially dependent density) and/or significant non-zero velocities (van Albada 1982; McGlynn 1984; Villumsen 1984; Aguilar & Merritt 1990; Theis & Spurzem 1999; Merrall & Henriksen 2003; Roy & Perez 2004; Boily & Athanassoula 2006). As we will see, it is precisely the fact that the system collapses by a large factor, allowing particles to reach very large velocities, that leads to the very significant energy ejection which we focus on. We will discuss, in the part of the paper on the mean-field approximation, some other very specific initial conditions. We will also consider in our conclusions the extent to which our study may be pertinent to other initial conditions.

We note also that these initial conditions are the most evident discretisation of the exactly uniform spherical collapse model, which is a reference point in the theory of non-linear evolution of self-gravitating systems in astrophysics and cosmology (see, e.g. Cooray & Sheth (2002)). The assumption usually made in using this model to predict the behaviour of physically relevant systems (e.g. in cosmology, via the formalism of Press and Schecter) is precisely that the total initial mass and energy are virialized. Our study shows that this is not a good approximation for this class of "almost" uniform spherical collapses.

Despite the numerical difficulties associated with these initial conditions, several extensive studies of them have, however, been reported in the literature, most notably a detailed study by Aarseth et al. (1988), and a more recent one reported in Boily et al. (2002). We will discuss these works in greater detail below, and use some of their results. Both works focus on how the singular collapse of the infinite N limit is regulated when there are a finite number of particles, and in particular the scaling observed in numerical simulations for the minimal size of the system[2]. Boily et al. (2002) also considers a wider class of non-spherical collapses, finding results to which we will return briefly in our conclusions. Our study can be seen as an extension of, and is complementary to, these studies, with which our results are in agreement. In more recent work Iguchi et al. (2005, 2006) have also studied collapse from such initial conditions, focussing on the properties of the virialized state. Although they do not consider the ejected energy quantitatively, these authors do remark on its potential importance in open systems. Some of the works cited above on collisionless relaxation (notably van Albada (1982); Aguilar & Merritt

[1] For recent studies see e.g. Arad & Johansson (2005); Arad & Lynden-Bell (2005), and also that of Levin et al. (2008).

[2] In the context motivating the study of Aarseth et al. (1988) the "points" are actually masses with extension (e.g. proto-stars) and the central question the authors wish to address is whether these masses survive or not the collapse of a cloud of which they are the constituents.

(1990); Roy & Perez (2004)) do include some quite cold uniform spherical initial conditions, with initial virial ratios of order 0.1, and note that there is significant mass ejection for this case. For the relatively small number of particles considered in these cases the energy ejection is, however, modest and does not strongly modify the final state, and the dependence of this quantity on particle number has not been explored[3]. We note also the studies in David & Theuns (1989); Theuns & David (1990), which explicitly discuss and model the ejection of particles ("escapers") from pulsating spherical systems.

We will describe here not only the dependence of the energies, and various other quantities, on N, but also detail the physical mechanism which leads to the ejection of mass. The probability of ejection turns out to be closely correlated with particles' initial radial positions, with essentially particles initially in the outer shells being ejected. The reason for this correlation is simply that these particles which are initially near the outer boundary systematically lag (in space and time) with respect to their uniform spherical collapse trajectories more than those closer to the centre[4]. These particles then gain the energy leading to their ejection in a very short time around the collapse time, as they pass through the time-dependent potential of the particles initially closer to the centre, which have already collapsed and "turned around". This lag, which has a very non-trivial dependence on the initial radial position, is manifestly a physical effect coming from the boundary: fluctuations to uniformity evolve differently depending on their position with respect to the boundary. Indeed the lag which leads to the mass ejection first develops at the outside of the system and propagates into the volume during the collapse phase. The importance of the finite size of the system in this respect is in contrast to the physics required to understand the scalings observed by Aarseth et al. (1988) and Boily et al. (2002). These can be understood by analyzing only the growth of fluctuations in the collapsing system in the approximation that it is of arbitrarily large size, which corresponds to the case of a matter dominated contracting universe. Nevertheless, as we will explain, we can use these arguments also to understand the scaling we observe of the ejected energy once the lag is assumed to be produced at collapse by the mechanism desribed above. While this is highly consistent with a description of the ejection phase which is clearly mean-field like — the lagging particles propapating through the time dependent potential of the rest of the mass — it is not, as we discuss, evident whether this is true of the physics involved in the development of the lag (and therefore determination of the ejected mass). In the final section we address more precisely what this mean field limit is, and how one should extrapolate numerically towards it. We then report some numerical tests on appropriate modifications of the initial conditions, which probe such convergence. While we establish that there is indeed good evidence for convergence, there are still measurable fluctuations due to non-mean field effects in macroscopic quantities such as the ejected energy at the largest particle numbers we have simulated.

The article is organized as follows. In the next section we recall the predictions for the N dependences of various quantities which follow from the uniform and perturbed spherical collapse model. In the following section we describe our simulations and principle results concerning the N dependence of the final state produced by violent relaxation. In Sect. 4 we investigate in detail the mechanism which leads to the ejection of mass and energy which we have observed. In Sect. 5 we discuss the validity of the Vlasov-Poisson limit in describing the evolution we have studied. Finally we give a summary of our findings and conclusions in the last section.

2 SCALINGS IN THE PERTURBED SPHERICAL COLLAPSE MODEL

In this section we recall basic results on the exactly uniform spherical collapse model, and then the scalings of physically relevant quantities (minimum attained radius, time of collapse, velocities at collapse etc.) which are obtained from a straightforward analysis of the evolution of perturbations to this model.

2.1 Uniform spherical collapse

The radial position $r(t)$ of a test particle in an (idealized) exactly uniform spherical distribution of purely self-gravitating matter of initial density ρ_0 and initially at rest (at time $t = 0$) is simply given by the homologous rescaling

$$r(t) = R(t)r(0) \tag{2}$$

where the *scale factor* $R(t)$ may be written in the standard parametric form

$$\begin{aligned} R(\xi) &= \frac{1}{2}(1 + \cos(\xi)) \\ t(\xi) &= \frac{\tau_{scm}}{\pi}\left(\xi + \sin(\xi)\right) , \end{aligned} \tag{3}$$

and

$$\tau_{scm} \equiv \sqrt{\frac{3\pi}{32G\rho_0}} . \tag{4}$$

At the time τ_{scm} the system collapses to a singularity. It will be useful in what follows to recall how the physical quantities diverge close to this singularity. Taking $\xi = \pi - \epsilon$ and expanding to leading order in ϵ gives $(t - \tau_{scm}) \sim \epsilon^3$, from which it follows that

$$R(t) \sim [t - \tau_{scm}]^{2/3} \tag{5}$$

and therefore the test particle velocities $v(t)$, proportional also to the initial radius $r(0)$, scale as

$$v(t) \sim [t - \tau_{scm}]^{-1/3}. \tag{6}$$

2.2 Perturbed spherical collapse

In this exactly uniform limit the evolution is independent of the size of the system, and the "particles" do not see its finite size (until the collapse). These solutions are thus formally valid as the radius of the system tends to infinity, and

[3] Aguilar & Merritt (1990) actually discount a possible systematic dependence on N in a footnote on page 36.

[4] We note that this formation of a "core-halo" structure during collapse is remarked on and briefly discussed by Aarseth et al. (1988). The link to mass/energy ejection are not, however, discussed in this article, or in Boily et al. (2002).

indeed they are precisely those for the evolution of an infinite contracting universe containing only matter, which are known to coincide with those derived in general relativity. The last equations given above then correspond to the behaviours in a contracting Einstein de Sitter (EdS) universe obtained when the curvature (corresponding to the initial cold start) is neglected.

The system we study here — N randomly placed particles in a spherical volume — can be treated, up to some time and at sufficiently large scales, as a perturbed version of this uniform limit. While in general the associated perturbations about uniformity will be expected to evolve in a way which will be sensitive to the finite size of the system, an approximation one can make is that such effects are negligible, i.e. to treat the perturbations as if they evolve also in an infinite contracting system. Quite simply this means we neglect the effect of the boundaries on the evolution of the density perturbations.

In the manner standard in cosmology (for the case of an expanding universe) one can then consider the fluid limit for the system and solve the appropriate equations perturbatively (see e.g. Peebles (1980)). In the eulerian formalism this gives, at linear order, a simple equation for $\delta(\mathbf{x})$, the density fluctuation (with respect to the mean density):

$$\ddot{\delta} + 2H\dot{\delta} - 4\pi G\rho_0\delta = 0 \tag{7}$$

where $H(t) = \dot{R}/R$ (dots denotes derivatives with respect to time) is the contraction ("Hubble") rate. These equations are derived in "comoving" coordinates $\mathbf{x} = \mathbf{r}/R(t)$, where $\mathbf{r}$ are the physical vector positions. Note that

$$R\,\dot{\mathbf{x}} = \dot{\mathbf{r}} - \dot{R}\,\mathbf{x}\,, \tag{8}$$

i.e., $R(t)\dot{\mathbf{x}}(t)$ is the velocity of the particle minus the velocity it would have in the limit of uniformity (in the cosmological context, the "peculiar" velocity with respect to the "Hubble flow").

It is straightforward (see Appendix A) to solve Eq. (7) by rewriting is as an equation for $\delta(R)$. In the limit $R \ll 1$,

$$\delta(R) \sim R^{-3/2} \tag{9}$$

i.e.,

$$\delta(t) \sim [t - \tau_{scm}]^{-1}\,. \tag{10}$$

This is simply the usual decaying mode of the expanding EdS universe, which becomes the dominating growing mode in the contracting case.

A much more detailed analytic treatment of perturbations to the spherical collapse model in the fluid limit, for the finite system, may be found in Aarseth et al. (1988). We give only the above results here, for the infinite radius limit, as they are the only ones we will make use of below.

2.3 Predictions for scalings

The singular behaviour of the spherical collapse is regulated by the fluctuations present at any finite N in the initial conditions we study. A simple estimate of the scale factor R_{min} at which one expects the spherical collapse model to break down completely may be obtained by assuming that this will occur when fluctuations at some scale (e.g. of order the size of the system) go non-linear. For Poisson distributed particles we have a mass variance (see e.g. Gabrielli et al. (2004))

$$\sigma^2(r) = \frac{\left(\langle N(r) - \langle N(r)\rangle\right)^2}{\langle N(r)\rangle^2} \propto \frac{1}{\langle N(r)\rangle}\,, \tag{11}$$

where the angle brackets denote an ensemble average over realizations. Using this as the initial normalisation of the density fluctuations, and the growth given in Eq. (9), we can infer

$$R_{min} \propto N^{-1/3}\,. \tag{12}$$

Using the scalings in Eqs. (5) and (6) it then follows that the maximum time t_{max} until which the spherical collapse model is a reasonable approximation is expected to scale as

$$[t_{max} - \tau_{scm}] \propto N^{-1/2}\,, \tag{13}$$

and the maximal infall velocity at any given radius as

$$v_{max} \propto N^{1/6}\,. \tag{14}$$

Note that we do not need to make explicit any scale in the argument to obtain this result: the scaling with N is obtained simply by taking the criterion that *some* amplitude is reached by the fluctuations at *some* fraction of the system size. In fact the result can be obtained on purely dimensional grounds: given that we are neglecting the finite size of the system, the only length scale in the problem — as gravity itself furnishes no scale — is given by the mean interparticle distance $\ell \propto N^{-1/3}$. Clearly then the length scale determined when R_{min} is combined with the size of the system must scale in this way, if the physical processes determining it are indeed independent of the size of the system.

Both Aarseth et al. (1988) and Boily et al. (2002) use simple, but equivalent, variants of the above argument to obtain these same scalings. In particular they can be formulated in terms of the spread in the collapse time of approximately spherical overdense and underdense regions, with initial amplitude fixed by Eq. (11). Or, alternatively, one can analyse the scaling of the pressure associated with growth of the peculiar velocities which must compensate the inward gravitational pressure to stop the collapse. One of the central findings of both Aarseth et al. (1988) and Boily et al. (2002) is that the scaling Eq. (12) is in fact observed, and we will verify again in our simulations that this is indeed the case.

The fact that these scalings are observed — and thus that the underlying approximation of (i) neglecting the boundaries of the system, and (ii) treating the fluctuations in the fluid limit, appears to work well — makes it instructive to compare collapsing spheres with different numbers of initially Poisson distributed particles at appropriately rescaled times. Let us consider two such spheres, with say N_1 and $N_2 > N_1$ particles, as if they were just two spheres of different radii (R_1 and $R_2 = R_1(N_2/N_1)^{1/3}$) evolving in an infinite collapsing universe with initially Poisson distributed points. In the approximation that the perturbations grow as given by linear fluid theory [i.e. as in Eq. (9) above], the sphere with N_2 points should be exactly equivalent, up to transients due to the cold start, to that with N_1 points at the initial time after the evolution of the scale factor brings its initially smaller density fluctuation (of amplitude $\propto N_2^{-1/2}$) to the initial larger amplitude ($\propto N_1^{-1/2}$) of the sphere with N_1 particles. This gives precisely the rescaling

inferred above, i.e., the different spheres should more generally — and not just at the time corresponding to R_{min} — be equivalent at scale factors rescaled in proportion to $N^{1/3}$. Deviations from equivalence in these rescaled time variables, on the other hand, must arise from physical effects not described by this approximation of neglecting the finite size of the system in its evolution up to collapse. We will thus compare below the different N systems at these different scales factors, and discuss to what extent the observed scalings of the ejected mass and energy can be understood in this simple approximation.

3 COLD SPHERICAL COLLAPSE: BASIC RESULTS FOR POISSONIAN FLUCTUATIONS

We describe in this section numerical results for evolution from initial conditions in which N particles are distributed randomly in a sphere, and given zero initial velocity. Besides reproducing known results for various quantities — notably the minimal collapse radius (or maximal potential energy), and the final profiles of the virialized structures — we present also our results for the N dependence of the ejected mass and energy.

3.1 Initial conditions and choice of units

Table 1 shows the names of the different simulations and the associated particle number N. The i-th realisation of an N particle configuration is thus labelled $PN - i$. The parameter ℓ is the *mean interparticle separation* in the initial configuration, defined as $\ell \equiv (3V/4\pi N)^{1/3} = R/N^{1/3}$ where V is the volume of the sphere of radius R. The *unit of length*, here and throughout the paper, is the *diameter of the initial sphere*, i.e., $R = 0.5$. The parameter m is the (identical) mass of the particles. The *unit of mass*, here and throughout the paper, is chosen *so that the initial mass density ρ_0 is unity*, i.e., $\rho_0 = mN/V = 6mN/\pi = 1$. Finally we take our *unit of time equal to τ_{scm}*, the uniform spherical collapse time as defined in Eq. (4) [5].

The parameter ε is the softening parameter introduced in the numerical integration, which we will discuss at length below.

3.2 Numerical code and parameters

We have performed numerical simulations using the publicly available code GADGET2 (`www.mpa-garching.mpg.de/gadget/right.html` 2000; Springel 2005). This code, which is based on a tree algorithm for the calculation of the gravitational force, allows one, in particular, as desired here, to perform simulations of a finite system with open boundary conditions. The two-body potential used is exactly the Newtonian potential for separations greater than the softening length ε, and modified at smaller scales to give a force which is attractive everywhere and vanishing at zero separation[6].

Name	N	ℓ	ε/ℓ	m
P512-1	512	0.63E-01	0.05	0.10E-02
P512-2	512	0.63E-01	0.05	0.10E-02
P512-3	512	0.63E-01	0.05	0.10E-02
P1024-1	1024	0.49E-01	0.065	0.51E-03
P1024-2	1024	0.49E-01	0.065	0.51E-03
P1024-3	1024	0.49E-01	0.065	0.51E-03
P2048-1	2048	0.39E-01	0.082	0.26E-03
P2048-2	2048	0.39E-01	0.082	0.26E-03
P2048-3	2048	0.39E-01	0.082	0.26E-03
P2048-4	2048	0.39E-01	0.082	0.26E-03
P2048-5	2048	0.39E-01	0.082	0.26E-03
P4096-1	4096	0.25E-01	0.10	0.13E-03
P4096-2	4096	0.25E-01	0.10	0.13E-03
P4096-3	4096	0.25E-01	0.10	0.13E-03
P8192-1	8192	0.25E-01	0.13	0.64E-04
P8192-2	8192	0.25E-01	0.13	0.64E-04
P8192-3	8192	0.25E-01	0.13	0.64E-04
P16384	16384	0.20E-01	0.16	0.32E-04
P32768-1	32768	0.16E-01	0.2	0.16E-04
P32768-2	32768	0.16E-01	0.2	0.16E-04
P32768-3	32768	0.16E-01	0.2	0.16E-04
P32768-4	32768	0.16E-01	0.2	0.16E-04
P32768-5	32768	0.16E-01	0.2	0.16E-04
P65536	65536	0.12E-01	0.25	0.80E-04
P131072	131072	0.99E-02	0.33	0.40E-05
P262144	262144	0.78E-02	0.41	0.20E-05

Table 1. Details of the simulations: N is the number of randomly distributed particles in a sphere of diameter taken equal to unity, ℓ is the average interparticle separation (see text for definition), ε is the softening length in the gravitational potential and m is the particle mass, in units in which the mean mass density is unity.

The values of the ratio ε/ℓ given in Table 1 correspond in fact to the single fixed value $\varepsilon = 0.0028$, i.e. the smoothing in this set of simulations is fixed in units of the initial size of the the system. Given that our aim here is to reproduce as closely as possible the evolution of the particle system (i.e. without smoothing), we will test carefully for the dependence of our results on the choice of ε, and, specifically, for their stability when ε is decreased compared to the value chosen in this set of simulations. As this discussion is closely related to the issue of the validity of the mean field (Vlasov Poisson) approximation to the dynamics of the system, we will present these results in Sect. 5, where we discuss this question. For now we note simply that if such a mean field approximation is valid, one expects that it should be sufficient that ε be significantly smaller at all times than the length scales relevant to this dynamics. We will see that the collapse phase leads to a minimal length scale of the structure of order the scale ℓ (and, as established by Aarseth et al. (1988) and Boily et al. (2002), proportional to this scale). Given the values for ε/ℓ shown in Table 1, it follows that the chosen ε is, in the largest N simulation, still smaller than this minimal collapse scale.

The large compression which the system undergoes as it

[5] In these units therefore $G = 3\pi/32$. In physical units τ_{scm} is approximately 2100 seconds if ρ_0 is 1g/cm^2.

[6] The exact expression for the smoothing function may be found in Springel et al. (2001).

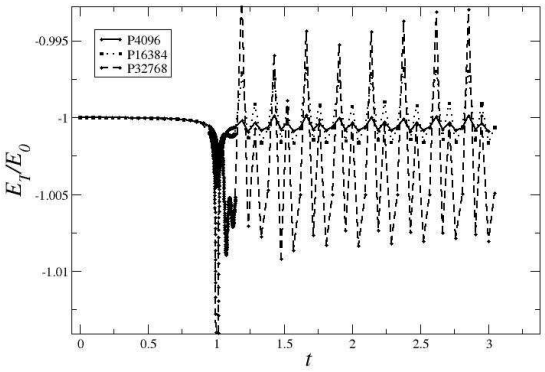

Figure 1. Total energy in the indicated simulations as a function of time.

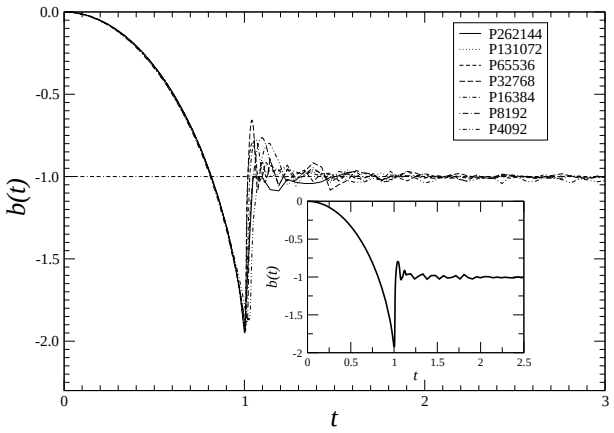

Figure 2. The virial ratio for the particles with negative energy [see Eq.(15)] as a function of time for different simulations. In the insert panel is shown a zoom of the behaviour after the collapse.

collapses requires that particular care be taken in choosing the numerical parameters which control the precision on the force calculation and time stepping. Given the physics of the system, we have used prescriptions for parameter choices in which we divide the entire range of times in three different phases. During the first ($0 \leqslant t \leqslant 0.95\tau_{scm}$) and the third ($1.14\tau_{scm} \leqslant t \leqslant 3.5\tau_{scm}$) we have used a relatively large time step (of the order of $5 \times 10^{-4}\tau_{scm}$) while in the collapse phase ($0.95\tau_{scm} \leqslant t \leqslant 1.14\tau_{scm}$ sec) we have used a more accurate time step (of the order of $5 \times 10^{-5}\tau_{scm}$). We have performed several tests to check the stability of the results given below, at the relevant level of numerical precision. We have in all cases quantified carefully the conservation of the total energy, which experience has shown to be a very sensitive quantity for monitoring the accuracy of the simulation (Aarseth 2003). Shown, for example, in Fig. 1 is the temporal evolution of the total energy E_T normalised to the initial energy E_0 in three of the simulations in Table 1. For larger N the energy is conserved less well, but the fluctuations are of less than one percent for all but the largest N. For the very largest N simulation in Table 1 the fractional error in the total energy reaches about 5% during the collapse phase. However, in this case and all the simulations, these variations in the energy are fluctuations about the total energy which do not lead to any measurable drift in the average value, which would be indicative of systematic error which propagates in time [7].

A further test of our simulations is their consistency with previous results reported in the literature for the same system, which we will discuss in the next subsection. We will then present our results for the dependence on initial conditions (i.e. on N) of the final virialized state.

3.3 Basic qualitative and quantitative results

Qualitatively the behaviour of this specific kind of cold collapse initial conditions is well known, and has been studied in detail in Aarseth et al. (1988) and Boily et al. (2002): the system collapses following approximately the spherical collapse solution until it reaches some minimal size, at a time of order τ_{scm}. It then "turns around" and rapidly (i.e. in a time considerably shorter than τ_{scm}) settles down to a quasi-stationary virialized state. This is illustrated in Fig. 2 which shows, for the simulations indicated (cf. Table 1), the evolution of the ratio

$$b(t) = \frac{2K^n}{W^n} \tag{15}$$

where K^n is the kinetic energy of the particles with negative energy, and W^n the potential energy associated with the same particles. The ratio represents the virial ratio of the entire system at early times, and that of the bound particles at late times.

A typical evolution of the radial density profile is shown in Fig. 3: until close to the maximal collapsed configuration, it maintains, approximately, the top-hat form of the original configuration and then in a very short time changes and stabilizes to its asymptotic form. We will discuss below in further detail this latter form and will also study in detail the deviations from the original form during the collapse phase.

Studies of the N dependence of the evolution have focussed mainly on the question of how the minimal size reached by the structure depends on this parameter. This minimal radius R_{min} may be defined in different ways, e.g., as the minimal value reached by the radius, measured from the centre of mass, enclosing 90% of the mass. Alternatively it can be estimated as the radius inferred from the potential energy of the particles, the minimal radius corresponding to the maximal negative potential energy[8]. The behaviour of R_{min}, determined by the first method, as a function of N is shown in Fig. 4. This observed behaviour is in good agreement with the prediction of the scaling Eq. (12), in accord

[7] The leap-frog time-integration method used by GADGET2 has, due to its simplectic nature, the property that it conserves extremely well — despite local fluctuations in time — the total energy of the system. For a detailed discussion see Springel (2005).

[8] Spherical symmetry is maintained up to a very good approximation until this time.

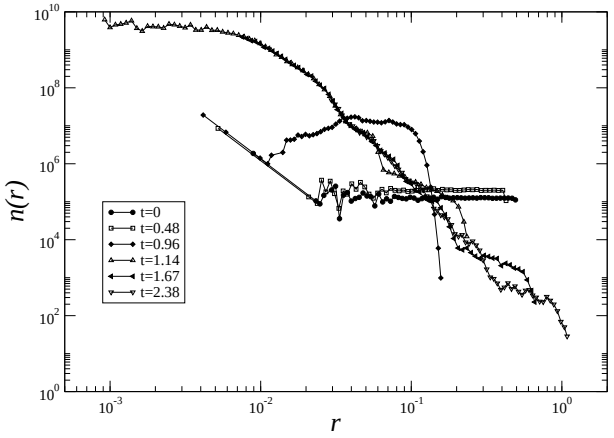

Figure 3. Density profile of particles with negative total energy at different times during the collapse, for the P65536 simulation.

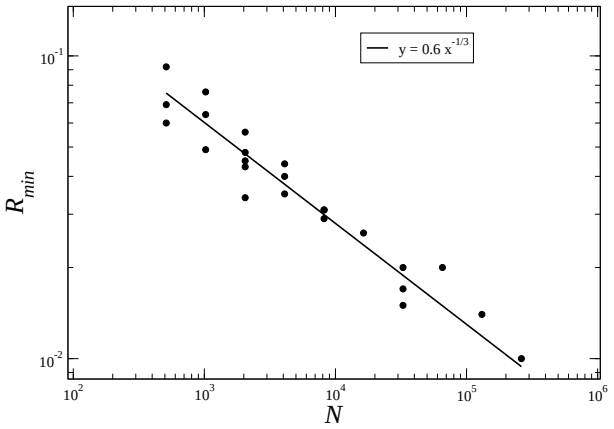

Figure 4. Behaviour of the minimal radius R_{min} attained, determined as described in text, as a function of N. The solid line is the best fit to the prediction of Eq. (12).

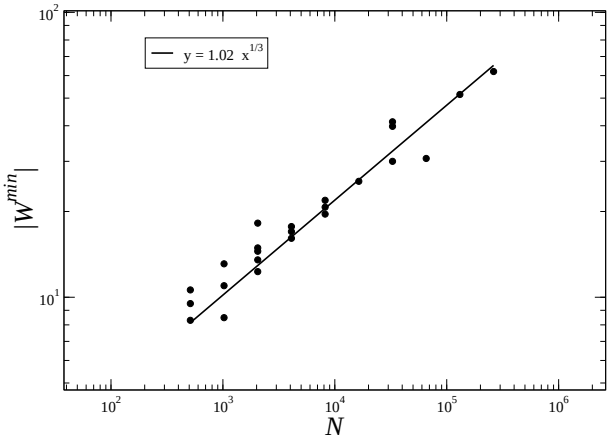

Figure 5. The absolute value of the minimal value reached by the potential energy (i.e. at the time $t = t_{max}$), as a function of N.

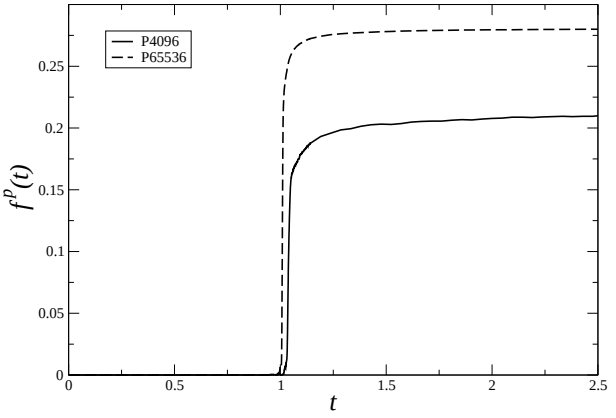

Figure 6. The behaviour of $f^p(t)$, the fraction of the particles with positive energy, as a function of time for two different simulations. A dependence on the number of particles is manifest.

with the findings of Aarseth et al. (1988) and Boily et al. (2002)[9]. We note that the factor of proportionality between R_{min} and ℓ is in fact almost unity (as in our units $\ell = 0.5/N^{1/3}$).

In Fig. 5 the absolute value $|W_{min}|$ of the potential energy at its minimum value, as a function of N. We again observe an excellent fit to the predicted behaviour.

3.4 N dependence of ejected mass

Our focus in this paper is on the presence of an ejected component of the mass, and energy, which has not been closely examined in these previous works. One of the features of the collapse and virialization is indeed that while all particles start with a negative energy, a finite fraction end up with a positive energy. Given that they move, from very shortly after the collapse, in the essentially time independent potential of the virialized (negative energy) particles, they escape from the system. Indeed at the times at which we end our simulations all such particles are very far from the collapsed region and move outward with almost constant energy, with a negligible probability of an encounter which could stop their escape to arbitrarily large distances.

This transfer of energy, which we will examine in detail below, occurs in a very short time around the maximal collapse, and depends on N. Both these facts can be seen in Fig. 6, which shows a plot of the fraction f^p of the particles with positive energy at any time.

Note that, while our simulations indicate that f^p attains a well defined asymptotic value, this is not expected to be the truly asymptotic value of this quantity, or of any of the other quantities we consider below: on much longer time scales than those considered here (i.e. the times characteristic of the violent relaxation of the system) further particles may gain energy and escape from the system, notably by two body encounters (see e.g. Binney & Tremaine (1994)). If the system is ergodic, simple considerations based on the microcanonical entropy (see e.g. Padmanabhan (1990)) imply that at asymptotically long times, and for an unsmoothed gravitational potential, the particles will tend to a configuration in which there is a single pair of particles with arbitrar-

[9] The latter paper finds that this result extend to N of order 10^7, an order of magnitude beyond the largest N we report here.

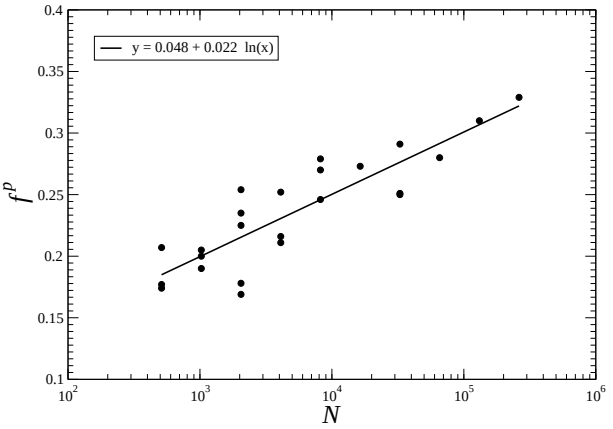

Figure 7. Behaviour of the fraction of ejected particles as a function of the total number of particles in the system. The solid line is the phenomenological fit given by Eq. (16).

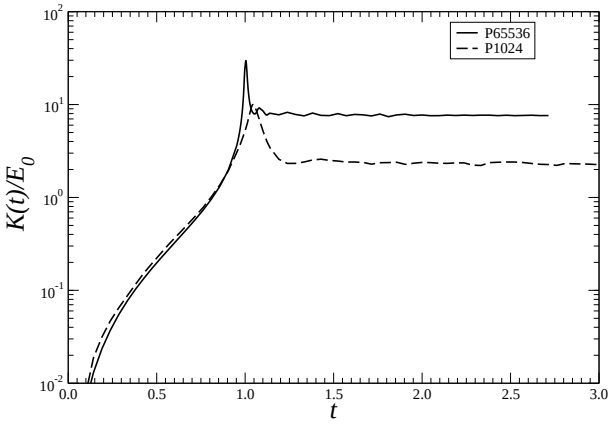

Figure 8. Behaviour of the total kinetic energy for two simulations with different number of particles.

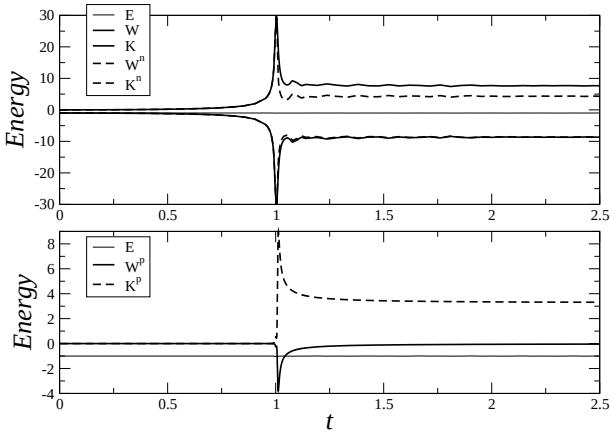

Figure 9. *Upper panel:* behaviour of the kinetic and potential energy, normalized in units of the absolute value of the initial energy, for all particles and for particles with negative total energy as a function of time for the P65536 simulation. *Lower panel:* The same for particles with positive total energy.

ily small separation, and the rest of the mass is in an ever hotter gas of free particles (see e.g. Aarseth (1974)). When the potential is smoothened, as in our simulations here, we would expect on such very long time scales to obtain a final state with some part of the mass bound and which depends strongly on this smoothing. We will, however, not explore this temporal regime here.

The N dependence of the asymptotic value of f^p we identify in this way is shown in Fig. 7. We note that, although determinations in different realizations of a given system with the same number of particles fluctuate, there appears to be a very slow, but systematic, increase as a function of N, which is reasonably well fit by

$$f^p(N) \approx a + b \log(N) \ , \qquad (16)$$

where $a = 0.048$ and $b = 0.022$. Alternatively it can be fit quite well (in the same range) by a power law $f^p \approx 0.1 N^{0.1}$.

3.5 N dependence of ejected energy

While the factor of the mass ejected varies, at most, very slowly with N, the energy it carries away has a much stronger dependence on N. In Fig. 8 is shown, for example, the behaviour of the total kinetic energy as a function of time in two simulations with different N. Not only the time at which the maximum is reached, but also the final value of the energy, change clearly[10]. We consider now carefully this dependence, and the related one of the potential energy of the different components.

In general the total energy, which is equal to the initial energy E_0, may be written as

$$E_0 = W + K = W^p + W^n + K^p + K^n + W^{p/n} \qquad (17)$$

where W (W^p, W^n) and K (K^p, K^n) are the total potential and kinetic energy of the particles (with positive energy, with negative energy) at the time t, and $W^{p/n}$ is the potential energy associated with the interaction of the particles with positive energy with those of negative total energy. Note that E_0 is simply, up to a correction from fluctuations due to the particle discreteness, the gravitational potential energy of a uniform ball of radius r_0, i.e., $E_0 = W(t=0) = -\frac{3}{5}\frac{GM^2}{r_0}$, where $M = mN$ is the mass of the ball (see e.g. Binney & Tremaine (1994)).

Shown in Fig. 9 are the evolution of these quantities[11]. The maximum of the kinetic energy K corresponds evidently to the minimum of the potential energy W. We see also that $W \approx W^n$, with only a very slight deviation around the time of collapse. This corresponds simply to the expulsion of the positive energy particles, which makes both W^p and $W^{p/n}$ completely negligible once these particles are far from the remaining bound part of the system.

Once the collapse phase is over, we therefore have to an excellent approximation

$$E_0 = W^n + K^p + K^n \ . \qquad (18)$$

[10] The common evolution of both curves is simply that predicted by the spherical collapse model, which leads to a divergence of the kinetic energy at τ_{scm}.

[11] The energies here and in subsequent figures, unless specified, are given in units of the absolute value of the initial total energy E_0.

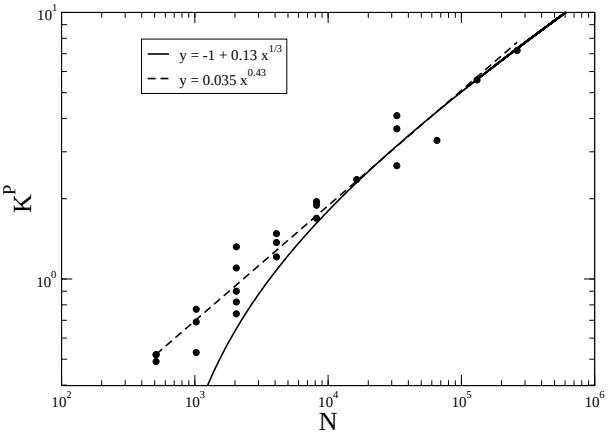

Figure 10. Behaviour of the total kinetic energy of the ejected particles (normalized to initial total energy) as a function of the number of particles in the system. The dashed line is the best fit to a single power-law behaviour for K^p itself, the solid line a fit to Eq. (20) with $W^n \propto N^{1/3}$, i.e. with W^n scaling exactly as W^{min} observed above.

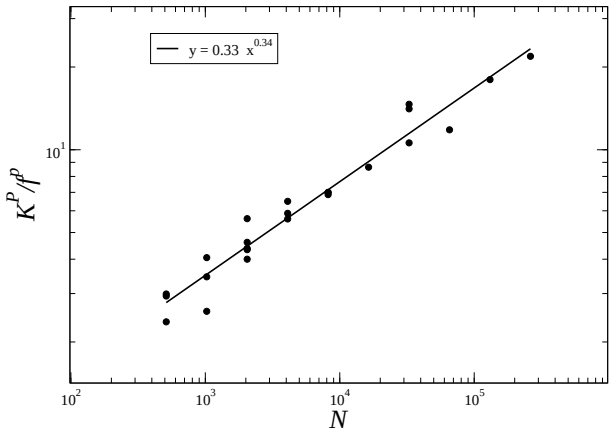

Figure 11. Observed behaviour of the ratio K^p/f^p for the set of simulations in Table 1.

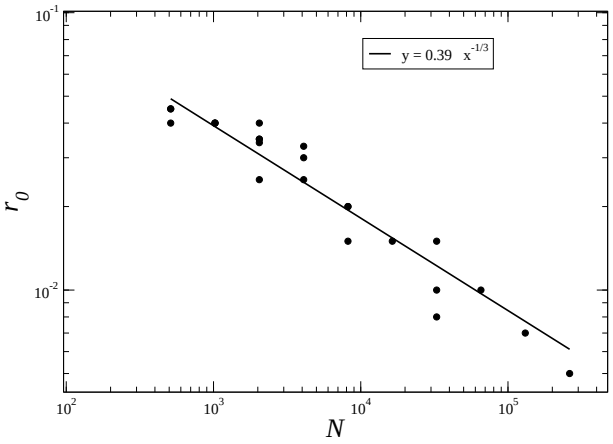

Figure 12. Behaviour of the parameter r_0 as a function of the number of particles in the simulation.

Further, since the bound particles rapidly virialize into a quasi-stationary state, we have

$$2K^n + W^n = 0\,. \tag{19}$$

The three non-zero energies K^p, K^n and W^n can therefore be expressed in terms of the initial (potential) energy E_0 and a single a priori unknown quantity, e.g., the ejected energy K^p.

Note that it follows from Eq. (19) and Eq. (18) that

$$E_0 = K^p + \frac{W^n}{2}\,, \tag{20}$$

so that for the case we are studying, in which $E_0 < 0$, these considerations do not on their own imply the necessity for energy ejection, i.e., one can satisfy Eq. (20) with $K^p = 0$. For $E_0 > 0$, however, the formation of a bound virialized stationary state requires such ejection.

In Fig. 10 we show the observed behaviour in our simulations of the total kinetic energy K^p of the ejected particles as a function of N. Two fits are shown: one is to a single power-law behaviour for K^p itself, the other to the behaviour which would be observed, using Eq. (20), if W^n scaled as W^{min} observed above. Thus in these curves we see a behaviour which is close to, but clearly different from, the simple scaling observed for W^{min}.

Shown in Fig. 11 is instead the ratio K^p/f^p, i.e., the kinetic energy *per unit ejected mass*, as a function of N. We observe that the simple behaviour $K^p/f^p \propto N^{1/3}$ provides a very good fit, with less scatter than in the previous plot. After we have discussed below in detail the mechanism of mass/energy ejection, we will give a simple scaling argument which accounts for this behaviour.

3.6 N dependence of density profiles

The radial density profile of the virialized structure formed by the bound particles after the collapse may be well fit in all our simulations by the functional form

$$n(r) = \frac{n_0}{\left(1 + \left(\frac{r}{r_0}\right)^4\right)}\,. \tag{21}$$

While the previous studies of exactly cold uniform initial conditions do not report results for this quantity, we observe that it is in agreement with that found for cold (i.e. low initial virial ratio) initial conditions in several previous studies (see e.g. Hénon (1964); van Albada (1982); Roy & Perez (2004)).

While the form of this profile is observed to be very stable in our set of simulations, the parameters n_0 and r_0 vary as shown in Figs. 12 and 13. Thus a good fit is given by the simple behaviours $r_0 \propto N^{-1/3}$ and $n_0 \propto N^2$. In Fig. 14 we show the density profiles for various simulations with different N where the axes have been rescaled using these behaviours.

These behaviours can be easily related to those we have observed in the previous section for f^p and K^p. Indeed using the ansatz of Eq. (21) it is straighforward to calculate both the number of particles $N^n = (1 - f^p)N$ which are bound, and the binding energy W^n of these particles [which is then related to K^p through Eq. (20)]. The first may be

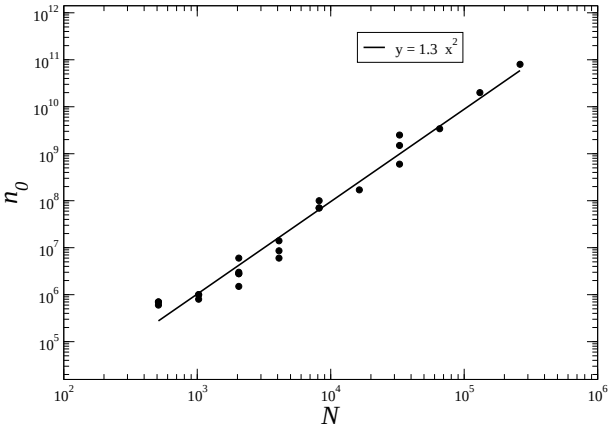

Figure 13. Behaviour of the parameter n_0 as a function of the number of particles in the simulation.

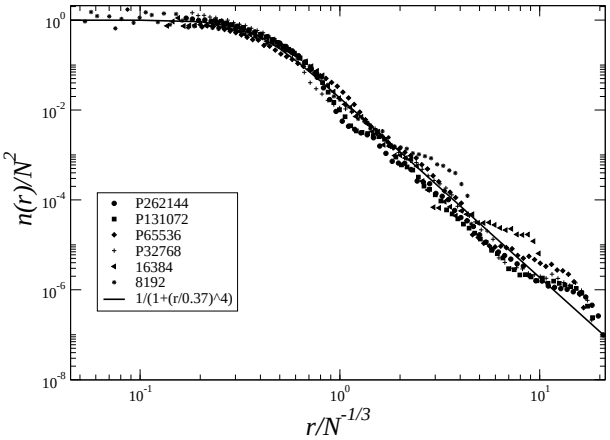

Figure 14. Density profile of the virialized structure at a time $t \approx 4\tau_{scm}$ for simulations with different number of particles. The y-axis has been normalized by N^2 and the x-axis by $N^{-1/3}$ (see text for explanations). The behaviour of Eq. (21) is shown for comparison.

determined analytically as

$$N^n = \sqrt{2}\pi^2 n_0 r_0^3 \tag{22}$$

while the second may be written as

$$W^n = -AGm^2 n_0^2 r_0^5 \tag{23}$$

where $A \approx 11$ is a numerically determined constant[12].

The fitted behaviours for r_0 and n_0 thus correspond, since $m \propto 1/N$, to $N^n \sim N$ (i.e. a constant bound mass, and therefore a constant ejected fraction of the mass f^p) and $W^n \sim N^{1/3}$ (and therefore $K^p \propto N^{1/3}$). Modifications of these fits consistent with the very slow variation of f^p described in the previous subsection can be given. Thus, to a good approximation, we simply find that the characteristic size of the final structure scales with N as R_{min}, the minimal radius attained in the collapse, does, i.e., in accordance

[12] For an isolated spherical system with a mass density profile $\rho(r)$ the potential energy is $-4\pi G \int_0^\infty M(r)\rho(r)rdr$, where $M(r)$ is the mass enclosed in the radius r.

N	t_1	t_2	t_3	t_4
131072	0.904	0.988	0.998	0.999
8192	0.666	0.952	0.988	0.998
512	—	0.809	0.953	0.993

Table 2. Times chosen for the different number of particles.

with the simple scaling argument which gives the prediction Eq. (12). Correspondingly the potential energy which is bound in this structure, given that the mass is approximately constant, increases in proportion to the inverse of this scale (and scales also as minimal value of the potential energy reached during the collapse).

4 MECHANISM OF MASS AND ENERGY EJECTION

In this section we consider in detail how the mass is ejected from the collapsing system.

4.1 The ejected particles

An evident starting point in considering the ejection of mass is to ask whether there is a direct correlation between a particle's initial radial position and the likelihood of its ejection, i.e., are particles preferentially ejected from the outside or the inside of the initial sphere?

Shown in Fig. 15 is the "radial rank correlation" [13]: at the indicated time t one ascribes a rank $n(t) \in [1, N]$ to each of the N particles according to their radial distance from the centre of mass, and then for each point one plots the couple $(n(t)/N,\ n(0)/N)$. The chosen times $t_1 ... t_4$ are not the same for the different N, but are as given in Table 2. This choice of the times is that discussed in Sect. 2.3 above, i.e., it corresponds to comparing the different simulations at times at which they are equivalent in the approximation — which leads, as explained in Sect. 2.3, to the predicted observed scaling of R_{min} — that they behave like infinite continuous systems with fluctations initially of amplitude proportional to $1/\sqrt{N}$, i.e., the times t' for the particle number $N' > N$ are determined by

$$f[R(t')]\frac{1}{\sqrt{N'}} = f[R(t)]\frac{1}{\sqrt{N}} \tag{24}$$

where $f(R)$ is the growth factor for perturbations, of which the full expression is given in Eq. (A3).

From these plots we see that that, while the strong correlation evidently present at early times tends to disappear, there is still some visible structure in the plot even at the final time, which corresponds to a scale factor just slightly larger than R_{min}, i.e., just a very short time before the maximal collapse. We do not show the plots for later times — after the collapse — as they are essentially identical to this last one. Given that typically of order twenty per cent of the

[13] This statistic has been introduced and used by Aarseth et al. (1988) to examine the degree of correlation of particles' radial positions with their initial radial positions. From their data for $N = 5000$ it is concluded that such correlation is very weak.

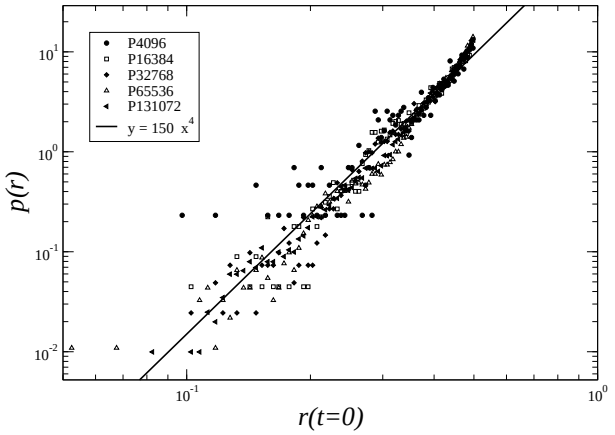

Figure 16. Normalized histogram (i.e. estimated probability distribution function) of the ejected particles as a function of their radial position in the initial configuration. The dashed line shows the best power-law fit.

mass is ejected, it thus appears that although ejected mass originates from all parts of the initial structure, it comes very preferentially from the outer regions of the sphere. Indeed the residual correlation in the plot appears to be a result solely of the correlation between ejection and initial radial position.

The degree of this correlation can be seen much more clearly in Fig. 16, which shows the estimated probability density function of ejection as a function of initial radius, i.e., the normalized histogram of the ejected particles as a function of their initial radius. In all the simulations we observe a very consistent behaviour, fitted approximately by a simple power-law:

$$p_e(r) \propto r^4 \,. \tag{25}$$

Given the uniform initial distribution, the probability that a particle is at radius r initially is proportional to r^2, so this result corresponds to a conditional probability of ejection

$$p(r) \propto r^2 \,, \tag{26}$$

i.e., the probability that a randomly chosen particle at radius r in the initial configuration will be ejected grows approximately as r^2. Thus, although some of the ejected mass comes from the inner parts of the initial sphere, there a very clear systematic correlation between initial radial position and ejection.

4.2 Development of lag during collapse

Since particles are preferentially ejected from the initially outer parts of the sphere, one would expect that their ejection may be related to a dependence of the evolution of particles prior to the collapse on their radial position. Indeed we have noted that the radial rank correlation plot of Fig. 15 at the last time shown, just before the collapse, is almost indistinguishable from that after the collapse. As we have discussed, however, in the uniform limit of the spherical collapse model (SCM), "particles" do not "see" the finite size of the system during the collapse phase, and indeed perturbations about the SCM in the continuum (fluid) limit may be treated in this same approximation that the collapsing system is infinite. With these approximations therefore the evolution of the trajectory of a particle cannot depend non-trivially on its initial radial position. As a corrollary such a dependence on radial position must arise necessarily from a coupling between the evolution of perturbations and the finite size of the system.

To quantify the difference in evolution of particles as a function of their initial radial position we consider the "lag", which we estimate as follows:

$$\Lambda(r,t) = \frac{1}{N(r)} \sum_{r \leqslant |\mathbf{r}'| \leqslant r+\delta r} \left(r'(t) - r'_{\rm SCM}(t) \right) , \tag{27}$$

where the sum is over the particles $N(r)$ initially at radial distance between r and $r+\delta r$ (with respect to the centre of mass), $r'(t)$ is actual radial distance at time t of the particle and $r'_{\rm SCM}(t)$ is the radial distance predicted at time t in the SCM, i.e., $r'_{\rm SCM}(t) = R(t)r'(0)$. The lag thus represents the average discrepancy between a particle's radial position and that in the SCM, as a function of radius.

The results for this quantity for different simulations and times — the same as those in the previous figure of the radial rank correlation — are shown in Fig. 17. For convenience of comparison $\Lambda(r,t)$ has been normalized to the radius $r_{\rm SCM}(t)$ of the sphere in the SCM model at the corresponding time t. We see that a net positive lag (i.e. net "stretching" of the positions with respect to their SCM values) develops initially for two quite separate ranges: for particles initially close to the centre, and for particles close to the outer boundary[14]. The reason for the development of systematically positive values is quite different in the two cases. For the particles close to the centre there is a systematic effect which makes the estimator necessarily biased towards positive values: once particles can deviate from their SCM radius by of order Δr, particles within this distance of the centre can reach the centre of mass, i.e., the minimal possible value of the radius, and thus their radius will start to increase again, which leads to an intrinsic asymmetry towards net positive values of $\Lambda(r,t)$ at these scales. From the corresponding plot in Fig. 15 we see that particles' radial positions with respect to the SCM indeed grow in the course of the collapse, with considerable redistribution of mass over the entire system already at the third time slice.

The clear positive lag which develops first close to the outer boundary, and then propagates progressively into the volume as time goes on, can be understood as follows. In addition to the mean field responsable for the SCM motion, the particles move under the effect of the field due to fluctuations which modify the SCM trajectories. These latter contributions are local, with the dominant contribution coming initially from nearest neighbour particles. For a shell at the outside of the volume, there is thus a difference compared to one in the bulk: as particles move around there is no compensating inward flux at the boundary for the mass which moves out under the effect of perturbations. Thus the net density of the outer shell decreases, and also the average density in the sphere at the corresponding radius, slowing

[14] Note that, since the mass inside the radius r grows in proportion to r^3, the fraction of the mass lagging in the two ranges is actually comparable even at the initial time despite the difference in radial range.

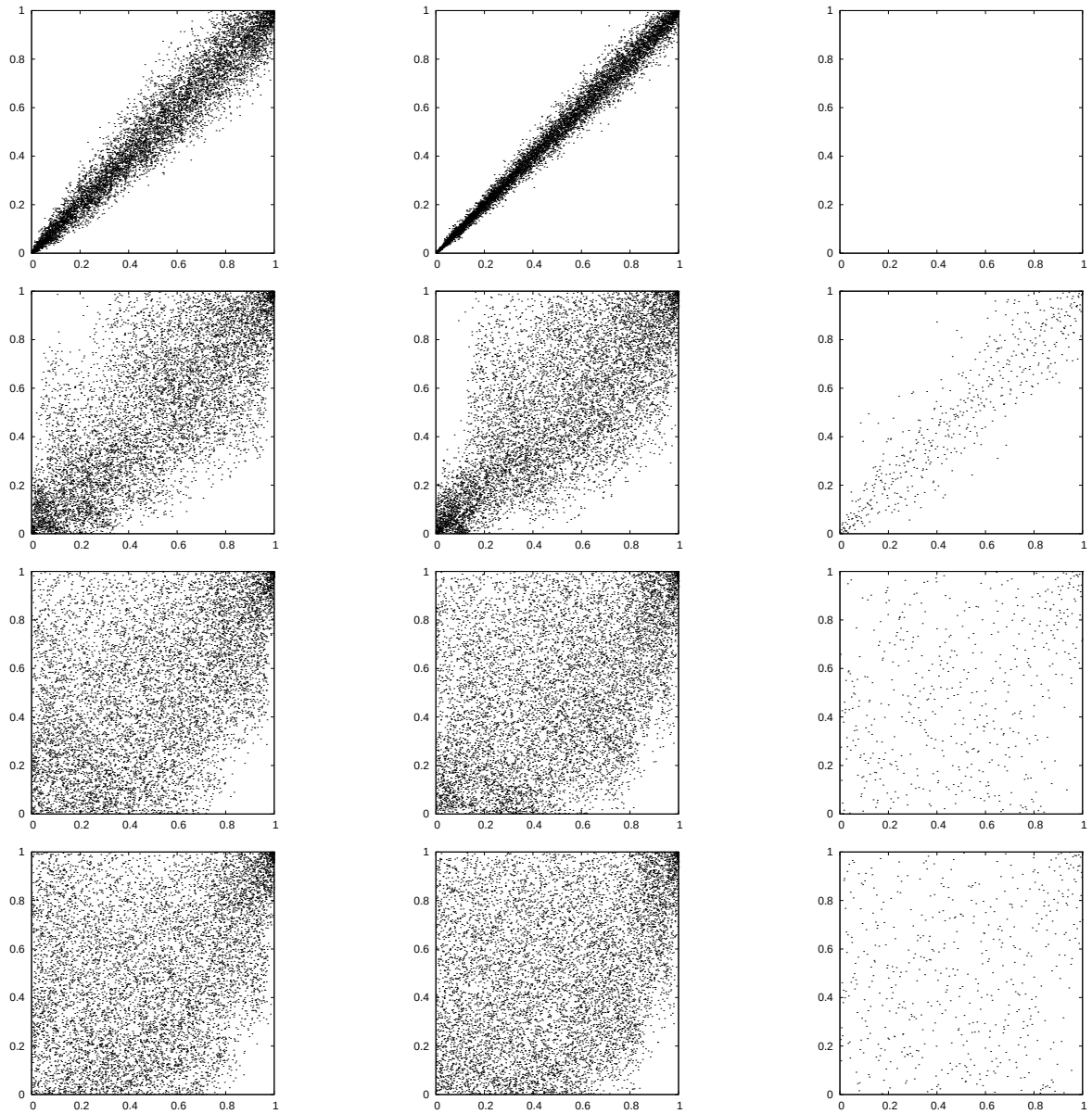

Figure 15. Radial initial rank (horizontal axis) versus rank at the times indicated in Table 2 for, from left to right, $N = 131072$, $N = 8192$ and $N = 512$ particles and, from top to bottom, the times t_1, t_2, t_3 and t_4. For the plots corresponding of the system with $N = 131072$ particles we have performed a random selection of 8076 particles.

its fall towards the origin[15]. As time goes on this asymmetry propagates into the volume: because the outer shells fall inward more slowly the mass in these shells stretches out radially, lowering the density further, which in turn "feeds" less flux into the shell. In the subsequent times in the figure we see clearly this effect, with a larger part of the outer mass lagging more and more compared to the SCM model, and, more significantly, compared to the mass closer to the centre. Indeed at the last time shown, just before the minimal collapse radius is reached, the lag is essentially constant — equivalent to a uniform dilatation of the whole sphere with respect to the SCM — for particles initially at radii less than approximately 0.8, but then rises sharply. The conclusion is that particles in the outer shells arrive at the centre of mass on average much later than those in the bulk.

4.3 Mechanism of mass ejection

That it is this "late arrival" of the outer parts of the sphere which leads to their net gain in energy and subsequent ejection can be seen from Fig. 18. It shows, for the P131072 simulation, the temporal evolution of the components of the mass which are asymptotically ejected or bound (i.e. with positive or negative energy a short time after the collapse has occurred). More specifically it shows the evolution of v_e

[15] We note again, as we did in the introduction, that the formation of a lagging low density outer region ("halo") during collaspe is noted in Aarseth et al. (1988), and a similar qualitative explanation for it is briefly outlined.

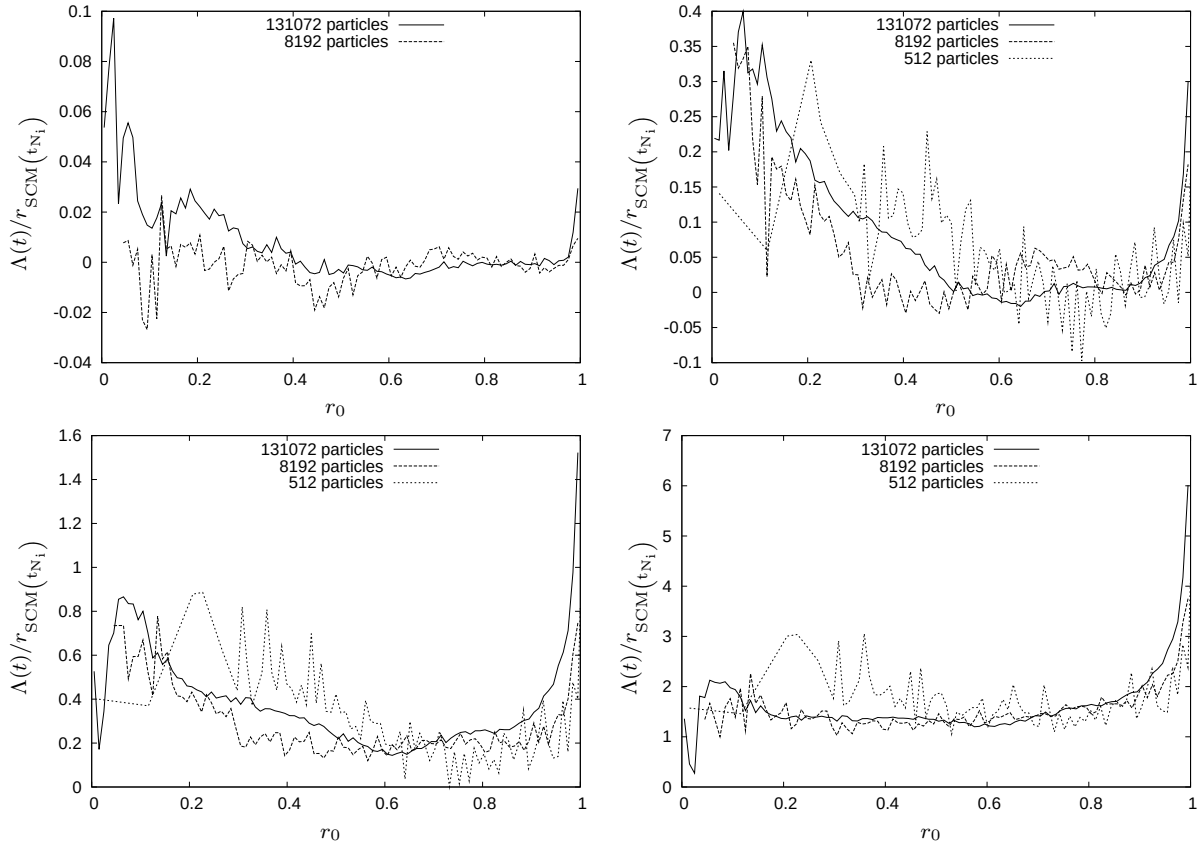

Figure 17. The "lag" as defined in Eq. (27), normalized as indicated, for the same four times as in the previous figure.

(and v_b) which is the average of the *radial* component of the velocity for the ejected (and bound) particles, and also e_e (and e_b) which is the mean energy per ejected (and bound) particle (i.e. the average of the individual particle energies). The behaviours of v_e and v_b show clearly that the ejected particles are those which arrive on average late at the centre of mass, with v_e reaching its minimum after the bound particles have started moving outward. Considering the energies we see that it is in this short time, in which the former particles pass through the latter, that they pick up the additional energy which leads to their ejection. Indeed the increase of e_e sets in just after the change in sign of v_b, i.e., when the bound component has (on average) just "turned around" and started moving outward again. The mechanism of the gain of energy leading to ejection is simply that the outer particles, arriving later on average, move through the time dependent *decreasing* mean field potential produced by the re-expanding inner mass. We note that a mechanism of this kind for "mean-field" mass ejection has been discussed in David & Theuns (1989) and Theuns & David (1990). Although we cannot quantitatively apply the results of these latter works to the present case — they treat the case of oscillations about a quasi-equilibrium — they give a qualitative insight into the ejection we observe.

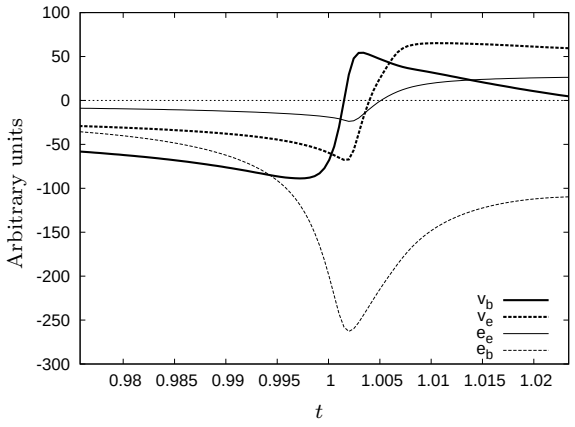

Figure 18. Radial velocity, and average energy per particle, as a function of time, of particles which are bound/ejected at the end of a $P131072$ simulation. The energy of the particles has been arbitrarily rescaled.

4.4 Scaling of ejected energy

Let us now finally attempt to be a little more quantitative, and relate this qualitative understanding of how the mass is ejected to the actual scaling we have observed of the ejected energy as a function of N.

To a first approximation the curves at the latest time plotted in Fig. 17 overlap, i.e., the profile describing the lag of the outer shells with respect to the inner ones is the

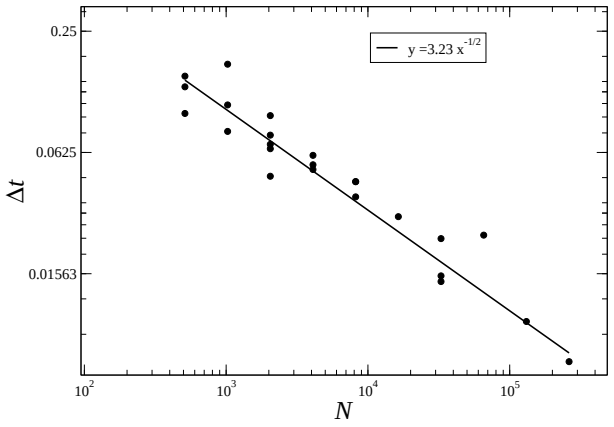

Figure 19. Time interval of the "peak" of the kinetic energy as a function of N.

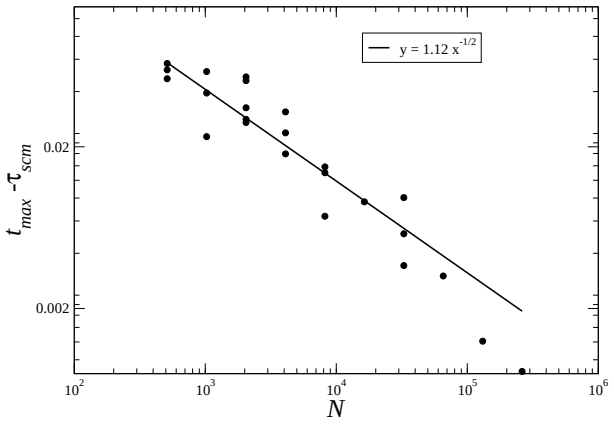

Figure 20. Time $t = t_{max} - \tau_{scm}$ as a function of N.

same. In this approximation all the simulations are therefore equivalent, up to rescalings of time and length, and would be expected to eject the same fraction of their mass if this ejection arises from the delay described by these curves.

A simple estimate of the energy E_g gained by the outer lagging mass as it passes through the inner core is then

$$E_g \sim \frac{W_{min}}{t_{char}} \times \frac{R_{min}}{v_{char}} \tag{28}$$

where the first term represents the rate of change of potential produced by the "core" structure, and the second the typical time for particles to cross it, where the parameters t_{char} and v_{char} are characteristic time and velocity scale for the process. We have seen already numerically that, to a very good approximation, $W_{min} \propto R_{min}^{-1}$, and therefore we have simply

$$E_g \sim \frac{1}{t_{char}} \times \frac{1}{v_{char}} \, . \tag{29}$$

We expect the role of t_{char} to be played by the typical time over which the "fall through" leading to the transfer of energy between the components occurs as we have described above. This can be estimated numerically, and its scaling with N inferred, from the data we have shown. For example, estimating it from the curve for the evolution of the total kinetic energy, which reaches a sharp peak as we go through this phase, as the temporal width at half the maximal value of the kinetic energy, we find the results shown in Fig. 19. As shown a very good fit is given by the scaling $\Delta t \propto N^{-1/2}$

The scaling of this characteristic time coincides with that predicted by the perturbed SCM model, as described in Sect. 2.3, for the difference $t_{max} - \tau_{scm}$, where t_{max} is the time at which the maximal collapse is reached. That this latter quantity also scales itself as predicted can be seen in Fig. 20.

The characteristic velocity v_{char} is that of the particles which will be ejected as they pass through the collapse, i.e., v_e in Fig. 18 above. We might anticipate that its scaling will also be predicted by the SCM for the maximal velocity reached at the collapse, [cf. Eq. (14) above], i.e.,

$$v_{char} \propto N^{1/6} \, . \tag{30}$$

That this is indeed a good approximation to the scaling can be seen in Fig. 21, which shows the same two radial velocities v_e and v_b as in the previous figure. Both axes of the plots for the curves from the $P512$ and $P8192$ simulations have been rescaled: the time axis as just described, and the velocities according to Eq. (30). We see that in these rescaled variables the evolution is indeed very similar.

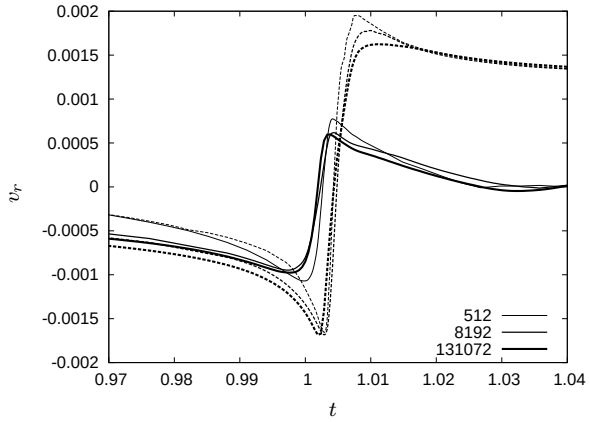

Figure 21. Radial velocity, as a function of time, of particles which are bound (solid lines) or expelled (dashed lines) at the end of the different simulations indicated. For the 8192 and 131072 simulations, the x-axis and y-axis have been rescaled as described in the text.

Taking these scalings to be exact, Eq. (29) then gives

$$E_g \sim N^{1/3} \, . \tag{31}$$

This simple estimate agrees quite well with the observed scaling of the ejected energy (i.e. asymptotic kinetic energy K^p of the positive energy particles). We have seen, however, that this scaling is followed more precisely by K^p/f^p, i.e., the energy ejected per unit mass, while f^p has a very weak (approximately logarithmic) dependence on N. The simple result obtained here has in fact been obtained with the assumption that the mass ejected is independent of N. Assuming the relevant properties for understanding the ejected energy are given by the curves for the lag shown in Fig. 17, this corresponded to the approximation that the curves at the latest time, just before the collapse, are the same for all N. In fact we can see that this is only true to a first approximation, and specifically that the integrated "lagging" mass

(i.e. under the curve) indeed appears to grow slowly as a function of N. Thus the scaling result obtained above can be adapted taking into account this increase as a function of N of the mass. We do not, however, have an analytical understanding of this observed N dependence of the lagging (and subsequently ejected) mass.

5 THE VLASOV POISSON LIMIT AND SENSITIVITY TO INITIAL CONDITIONS

5.1 Definition of the Vlasov Poisson limit

We now discuss the extent to which the evolution of the simulated system is "collisionless", i.e., described by the coupled Vlasov-Poisson (VP) equations (or "collisionless Boltzmann equation"). The latter should describe the evolution of the system in an appropriate $N \to \infty$. The naive such limit applied here, i.e. $N \to \infty$ Poisson distributed particles, is clearly not the desired limit, as it converges to the singular SCM. Indeed we have explicitly identified macroscopic N dependences in various quantities, which diverge if we perform this naive extrapolation.

Existing formal proofs of the validity of the VP limit (Braun & Hepp 1977) for a self-gravitating system require, however, that the singularity in the gravitational force at zero separation be regulated when the limit $N \to \infty$ is taken[16]. Incorporating such a modification of the force will clearly regulate the divergence in the SCM as we converge to the uniform mass distribution. One would then expect to obtain, for sufficiently large N, a final state which is well defined and N independent, but strongly dependent on the implementation (and scale) of the regulation.

This limit also is not the VP limit relevant here: while we have indeed introduced such a regulation of the force (characterized by the smoothing ε), we have done so, as discussed in Sect. 3, for reasons of numerical convenience. Indeed, as we have discussed, our criterion for our choice of ε is that it be sufficiently small so that our numerical results are independent of it, and we interpret our results as being representative of the limit $\varepsilon = 0$. In Fig. 22 are shown, for example, the evolution of the fraction of particles with positive energy as a function of time for the different indicated values of ε. Other quantities we have considered show equally good convergence as ε decreases. Note that for the given simulation (cf. Table 1), the mean interparticle distance $\ell = 0.016$, so that the convergence of results is attained once ε is significantly less than ℓ. As we have seen, the minimal size reached by the collapsing system scales in proportion to ℓ (with a numerical factor very close to unity, as can be seen in Fig. 4). We interpret the observed convergence as due to the fact that the evolution of the system is determined primarily by fluctuations on length scales between this scale and the size of the system. Once ε is sufficiently small to resolve these length scales at all times, convergence is obtained.

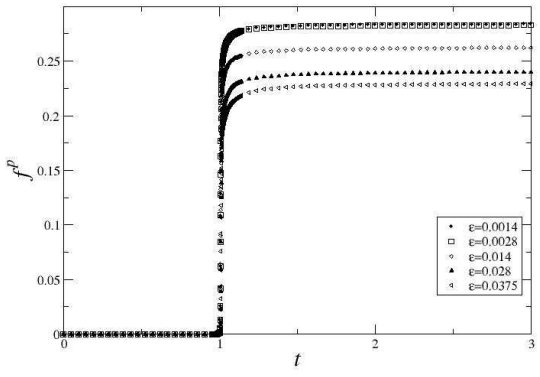

Figure 22. Evolution of the fraction of the mass with positive energy for simulations with $N = 32768$ for the different values indicated of the smoothing parameter ε.

A different, less rigorous but more physically intuitive, derivation of the VP limit is given (see e.g. Buchert & Dominguez (2005)) by a coarse-graining of the exact one particle distribution function over a window in phase space. The VP equations are obtained for the coarse-grained phase space density when terms describing perturbations in velocity and force below the scale of the coarse-graining are neglected. A system is thus well described by this continuum VP limit if the effects of fluctuations below some sufficiently small scale play no role in the evolution. The validity of such an assumption for our system is indicated by precisely the kind of behaviour we have just noted of our results as a function of ε.

5.2 Numerical extrapolation to the VP limit

The VP limit defined in this way thus corresponds to taking $N \to \infty$, while *keeping fixed the initial fluctuations above some scale*. The validity of this limit for our system may be explored numerically by defining such an extrapolation and studying stability of our results to it. This can be done as follows: starting from a given Poissonian initial condition of N particles in a sphere of radius R, we create a configuration with $N' = nN$ particles by substituting each particle by n particles in a cube of side $2r_s$ centred on the original particle. The latter particles are distributed randomly in the cube, with the additional constraint that their centre of mass is located at the centre of the cube (i.e. the centre of mass is conserved by the "splitting"). In this new point distribution fluctuations on scales larger than r_s are essentially unchanged compared to those in the original distribution, while fluctuations at and below this scale are modified[17]. We have performed this experiment for a Poisson initial condition with $N = 4096$ particles, splitting each particle into eight ($n = 8$) to obtain an initial condition with $N' = 32768$

[16] This proof is given in a finite volume. We do not believe that this is an important difference here, as the dynamics we describe will be modified in a quite trivial way, on the time scales considered, if we put our system in a box: the ejected component will simply bounce off the walls and remain as an unbound cloud moving in and out of the time independent potential of the "core".

[17] See Gabrielli & Joyce (2008) for a detailed study of how fluctuations are modified by such "cloud processes".

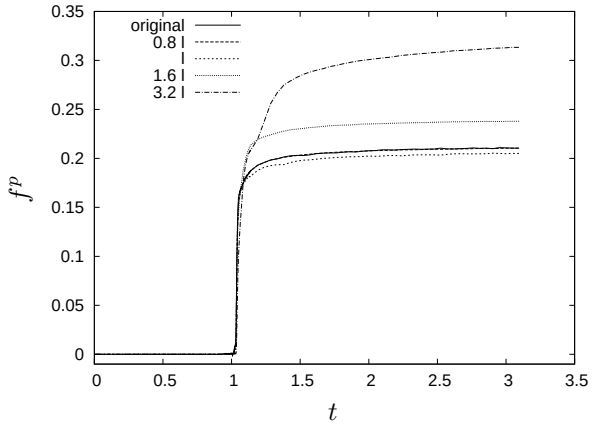

Figure 23. Evolution of the fraction of particles with positive energy as a function of time, for the different indicated values of the parameter r_s described in text. The "original" initial conditions has 4096 particles while the others have 32768 particles. Note: the curve for 0.8ℓ is not visible because it is superimposed on that for the "original" one .

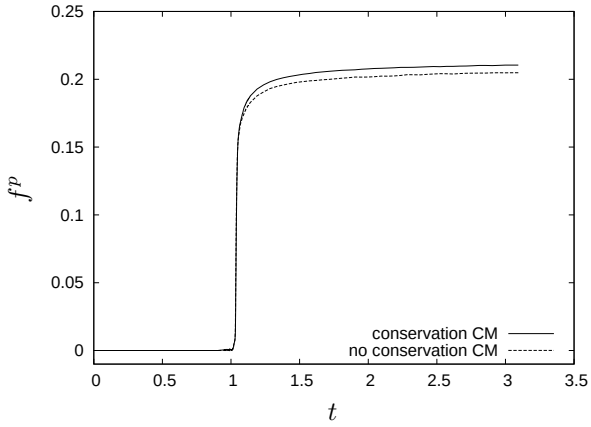

Figure 24. Evolution of the fraction of particles with positive energy as a function of time, from initial conditions given by the "split" configurations described in text. The results are for a Poisson configuration with $N = 4096$ split into one with $N' = 32768$ particles, and $r_s = 0.8\ell$, and differ only in whether the centre of mass of the split particles is conserved or not.

particles. Results are shown in Fig. 23 for the ejected mass as a function of time, for a range of values of the parameter r_s, expressed in terms of ℓ, the mean interparticle separation (in the original distribution). While for $r_s = 0.8\ell$ the curve of ejected particles is indistinguishable in the plot from the one for the original distribution, differences can be seen for the other values, greater discrepancy becoming evident as r_s increases. This behaviour is clearly consistent with the conjecture that the macroscopic evolution of the system depends only on initial fluctuations above some scale, and that this scale is of order the initial interparticle separation ℓ. And, as anticipated, this translates into an N independence of the results when N is extrapolated in this way for an r_s smaller than this scale.

The observed behaviour of the ejected mass for the larger values of r_s can be understood as follows: for an initial Poisson distribution, after dividing each particles following the procedure described above, the distribution remains Poissonian at large scale. Therefore the growth of fluctuations inside the sphere and hence the radius of minimal collapse, etc., will be the same for the original and the new simulation. The relevant difference between the initial conditions of the two simulations are for radius $r > R - r_s$ in the original distribution, because particles situated in this region have a strong probability to lie outside the original sphere in the split distribution. These particles will lag strongly because they feel a weaker effective gravitational field than the ones inside the sphere and a large number of them will be ejected, explaining the strong increase of ejected particles as r_s increases.

5.3 Sensitivity to initial fluctuations at large scales

It is interesting to probe further the sensitivity of the results to the initial fluctuations over the range of scales which appear to be relevant to the determination of the final state. In Fig. 24 are shown the same quantity as in the previous figure, for $r_s = 0.8\ell$, with the only difference that the n points are now distributed *randomly* in a cube of side $2r_s$ both with and without the constraint that the centre of mass be conserved. Without the constraint there is an additional random displacement of the mass, which induces slightly greater fluctuations at large scales, and specifically a non-zero fluctuation in the dipole moment of the whole mass distribution[18]. We see that, although this corresponds to an extremely small modification of the fluctuations at large scales, it leads to a perceptible change in the final macroscopic properties.

Finally we can probe the dependence on initial fluctuations at different scales by comparing the evolution from the Poissonian initial configuration, to that from initial "shuffled lattice" configurations with the same number of particles. The latter are generated by placing particles on a perfect lattice, and then subjecting them, independently, to a random displacement in a cube of characteristic size δ_s. A sphere containing the required number of particles is then extracted, with centre on a lattice point. If the scale δ_s is or order the interparticle distance or larger, the latter distribution has then, up to this scale, fluctuations which are Poissonian (and identical in amplitude to those in the initial Poissonian distribution), while at larger scales it has fluctuations of a much lower amplitude than in the latter distribution. In Figs. 25 we show the evolution of the fraction of the ejected mass as a function of time, for the indicated values of the parameter δ_s, for configurations with 4143 particles. In comparison with the Poisson configurations we have reported above with approximately the same number of particles (4096), which eject $20 - 25$ percent of their mass, the mass ejected is significantly larger in all cases, increasing monotonically as δ_s decreases. This is in line with what everything we have seen above: for any $\delta_s \leqslant 1$ the fluctuations

[18] For an infinite point distribution (see, e.g. Gabrielli et al. (2004); Gabrielli & Joyce (2008)) the constrained case produces long wavelength fluctuations with a power spectrum decaying in amplitude in proportion to k^4 (where k is wavenumber), while the unconstrained "shuffling" produces a power spectrum proportional to k^2.

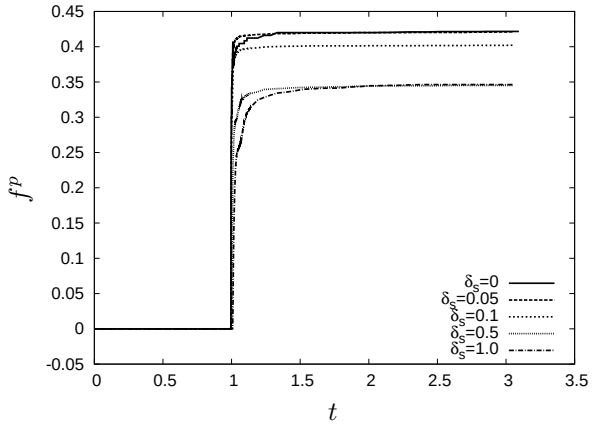

Figure 25. Evolution of the fraction of particles with positive energy as a function of time, for simulations from "shuffled lattice" initial conditions with different values of the parameter δ_s.

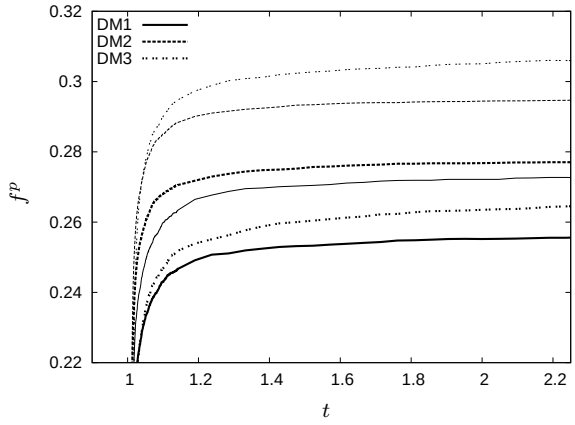

Figure 26. Evolution of the fraction of particles with positive energy for the different indicated initial conditions (see text). In each case the thick line corresponds to the heavier particles (mass m_1) and the thin line to the lighter particles (mass m_2).

at relevant scales are smaller than those in the Poisson distribution, and their amplitude decreases as δ_s does. For the limit case of a perfect lattice (i.e. $\delta_s = 0$), the collapse is the most violent. Indeed in this case the only density fluctuations regularizing the collapse are surface fluctuations (associated with the finite size of the system), and close to half (43%) of the initial mass is ejected.

5.4 Further test for non-VP effects

A useful test for non-VP effects is to use particles of different masses in the simulations: given that the VP limit is essentially a mean field approximation, the trajectories of particles should be independent of their mass if it is valid. There should therefore be no segregation (up to statistical fluctuations) between the different species in the final configuration if this limit applies. We have thus run three simulations with dispersion in particles' masses: we denote by DM1 and DM2 two realizations of an $N = 4096$ Poissonian initial condition, in which we have assigned, randomly, a mass $m_1 = 4/3m$ to half of the particles, and $m_2 = 2/3m$ to the other half. Finally, we denote by DM3 the same realization as DM2 (i.e. with particles in the same positions), but now with half of the particles with masses $m_1 = 20/11m$ and the other half $m_2 = 2/11m$. In Fig. 26 we show the fraction of ejected particles for the three simulations. Firstly we observe that the difference between the number of light (m_2) and heavy (m_1) particles is, albeit larger in DM3 than in DM1 and DM2, in all three cases of order the dispersion in the average number ejected in different realizations (see also Fig. 7). The difference in the number ejected of each species in a given simulation (with given density fluctuations) is, however, too large to be a purely statistical fluctuation, and indeed we see that there are systematically more light particles ejected than heavy ones, with a clearly more pronounced effect as the mass difference increases. This small excess of lighter ejected particles can naturally be attributed to the ejection of some (small) part of the mass by two-body collisions, rather than by the mean field mechanism described in the previous section: such collisions modify the energy per unit mass, which is the relevant quantity in the mean field limit, in a different way according to their mass. In a collision between a light particle and a heavy particle, notably, the trajectory of the former is deviated much more than that of the latter, and therefore it is more likely to be ejected[19].

6 CONCLUSIONS AND DISCUSSION

We have studied in this article the collapse and violent relaxation of N (classical Newtonian) self-gravitating particles, initially at rest and distributed randomly in a sphere. We have focussed on the characterisation of the macroscopic properties of the quasi-stationary virialized state which results, and in particular on the mass and energy of the bound and ejected components. We have identified unexpected non-trivial dependences of the latter on N, where the latter varies over approximately three orders of magnitude (from a few times 10^2 to a few times 10^5). We have studied in detail the evolution through the collapsing phase, identifying the physical mechanism leading to this mass and energy ejection. Further we have used this to give a simple analysis which allows one to explain the observed scaling with N of the energy per unit ejected mass ($\propto N^{1/3}$). Finally we have clarified how one can test the hypothesis that the evolution is representative of the Vlasov-Poisson limit by an appropriate extrapolation of the particle number. While our main convergence test show good stability of results, another one allows us to detect residual non-zero effects corresponding to deviation from this limit.

One point which we emphasize is that we have *not* explained, even qualitatively, the very slow (approximately logarithmic) growth with N of the fraction of the mass ejected f^p. We note that this result is numerically less robust than the result for the energy: the effect is both very small over the range of N simulated, and also shows greater fluctuations from realization to realization than for the energy

[19] Such mass segregation effects have been observed also in Aarseth (1974) in the ejection by two body collisions which occurs as such systems relax on much longer time scales than those considered here.

per unit mass. Indeed in Fig. 7 we see that if we omit the two points with largest N, the results would be quite consistent with a convergence of the ejected mass to a constant value. As these largest N simulations are those we have not been able to test for discreteness effects using the tests we have discussed (which require extrapolation to still larger N), we cannot exclude that the apparent continued growth might be due to such effects. Indeed we note the growth of the ejected mass with N cannot be consistently extrapolated by a logarithmic (or power law) dependence to arbitrarily large N, as it is a quantity which is bounded above (by the total mass). The numerical results we have given, despite the fact that we have considered a very large number of particles, thus do not actually resolve the asymptotically large N dependence (or asymptotic constant value) of the ejected mass, or indeed that of the ejected energy (or the associated virialized state) is. Further numerical study, with larger simulations, would be feasible for groups with greater numerical resources than ours, and might resolve the issue[20]. It is natural to expect that the slow growth in the mass will reach an upper bound when the fraction of mass becomes of order the total mass. We remark that a $\log N$ behaviour, for example, could be explained if the quantity of mass which "lags" as we have described, and is then ejected, grows exponentially in the course of the evolution from a fluctuation which is originally of order $1/N$ (or some power thereof). One would expect the growth law to change, and flatten to a constant, when the fraction of lagging mass becomes of order one half.

In relation to this last point it is interesting also to consider a little further the case of an initial lattice-like configuration, which we discussed briefly in Sect. 5.3. These are, as we have noted, much more uniform configurations in the range of scales which are relevant to the macroscopic evolution, and indeed we observed considerably larger mass ejection. This corresponds, as one would expect, also to a more violent collapse, with larger energy ejection. We show, for example, in Fig. 27 the evolution of the total kinetic energy for the different values of δ_s (the "shuffling" of the lattice) indicated. The increasing violence of the collapse is evident as δ_s decreases. We note that, for sufficiently small δ_s, the maximal collapse (corresponding to the maximum of the kinetic energy) actually occurs *before* the time predicted by the uniform SCM. This is in contrast to the behaviour for all the Poissonian initial conditions we have considered, which in all cases gave a collapse time longer than τ_{scm} (cf. Fig. 20). In the latter case this behaviour can be understood in terms of the lagging mass we have discussed, which leads to the system having a lower effective mean density (and therefore a longer collapse time). That a different behaviour occur for the exact (or near exact) lattice, may be indicative that a quite different behaviour of the Poissonian system may be reached when N is extrapolated sufficiently far that, like in the exact lattice, a regime is reached in which the dominant fluctuations are those arising from the finite size of the system. A naive extrapolation of the N dependence of f^p for the Poissonian configurations to the value observed for the lattice gives $N \sim 10^7$. To resolve this point it would evidently be interesting to study the evolution from

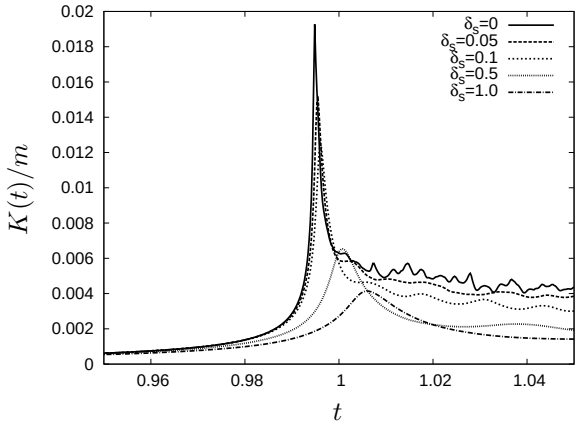

Figure 27. Evolution of the kinetic energy as a function of time, for the shuffled lattice initial conditions with the indicated values of δ_s.

these initial lattice or lattice-like configurations, and indeed other very uniform configurations such as those described in Hansen et al. (2007), in more detail, and for larger particle number[21].

What, otherwise, have we learnt from this study? The following points seem pertinent to us:

- Analyses of violent relaxation usually neglect the effects we have focussed on here, and assume that energy and mass of the final virialized system is equal to that of the initial configuration. This is true, for example, of the use of the spherical collapse model in the context of cosmology (see e.g. Cooray & Sheth (2002)). While it may be, in this context, a good approximation to neglect ejected mass — generically we would not expect to have the very large collapse factors observed here which are closely linked to this ejection — the non-trivial slow N dependences we have seen would urge some caution in this regard. Further in theoretical attempts to understand the properties of the virialized states, the same approximation is generically made. An evident example is the famous proposal by Lynden-Bell (1967) that the result of violent relaxation should be a state which maximizes a coarse-grained entropy in phase space subject to the constraints of the VP equations, and notably total energy and mass conservation. What we observe in our simulations is that the density profile of the final state (and also velocity distributions, which we have not reported here) is very robust while the conservation of the energy and mass of the initial state appears to be of little relevance. This observation may be important in attempts to understand the properties of these states, and in particular their dependence (or non-dependence) on initial conditions.
- Our study shows that the assumption that the evolution of such systems on these timescales is fully represented by the VP (or collisionless) limit should also be treated with some caution. In our simulations we have found small, but significant, non-VP effects with a simple mass segregation test. In any case it is important to define clearly the appro-

[20] Boily et al. (2002) gives results for a spherical collapse with 10^7 particles (but does not report the ejected mass and energy)

[21] As the cost of numerical integration depends, essentially, on the violence of the collapse, we reach our limit for the exact lattice at a particle number of order that reported (N=4143).

priate extrapolation to the VP limit, which we have seen may be less trivial than one might naively appears. We believe the extrapolation we have defined here — in which particle number increases while the fluctuations above some scale are held fixed — is the appropriate one for this system.

• Our results suggest that open self-gravitating systems may be able, theoretically, to eject an arbitarily large amount of energy on a *dynamical* time scale. This effect is reminiscent of the "gravothermal catastrophe", and indeed its origin is the same: because the gravitational potential is unbound below, an arbitrarily large kinetic energy can be gained by making some mass arbitrarily bound. The mechanism, however, and timescale, are completely different. It is clear that the ejection we have seen is related to the collapse, which in turn is related to the spherical symmetry of the problem we have considered. What about more general initial conditions? We note that, although we expect smaller collapse factors for a generic initial condition, very large collapse factors may occur for non-symmetric initial conditions. This question has been considered at length in Boily et al. (2002), which presents a detailed numerical study of the generalisation of the fluid SCM to axisymmetric and triaxial configurations. In the former singularities remain intact, and a relation $R_{min} \propto N^{-1/6}$ is found empirically to replace the $R_{min} \propto N^{-1/3}$ behaviour of the spherical case. In the triaxial case the collapse factors are found to be typically finite, but they can be very large and no upper bound is placed on them.

The study we have presented is a purely theoretical one of an idealized problem. It is interesting, of course, to consider whether, in particular, the "explosive" ejection of energy we have found could have any direct relevance to real physical systems or realistic models of them in astrophysics or cosmology. For the former context it is relevant to consider the validity of the Newtonian limit which we have treated. To do so it is useful to write the ejected kinetic energy as

$$K^p \sim N^{1/3} \frac{\Phi_I}{c^2} \times M_I c^2 \tag{32}$$

where Φ_I and M_I are, respectively, the initial mass and (Newtonian) gravitational potential, and c is the speed of light. The first factor is, in fact, approximately the maximal value reached by the potential, and if this is small compared to unity we expect the Newtonian approximation to be valid. Thus our determination of K^p would be expected to remain valid until this energy reaches of order the evident upper bound imposed by the rest energy of the ejected mass (which is of order that of the initial mass). We note also that if the initial radius of the sphere is R_I the Newtonian approximation can remain valid at all times provided the number of Poisson distributed masses satisfies

$$N \ll \left(\frac{R_I c^2}{G M_I} \right)^3 . \tag{33}$$

Thus, for example, if M_I and R_I are taken to be a solar mass and radius, respectively, the Newtonian approximation should be valid at all times during the collapse if $N < 10^{14}$, i.e., if the mass of the initially Poisson distributed "particles" is greater than about 10^{-14} solar masses. Normalizing the ejected energy using our simulations above, one would obtain an ejected energy of about 10^{49} ergs for the largest value of N we reported ($N \approx 2 \times 10^5$), and, extrapolating our results, an energy as large as that of a typical supernovae ($\sim 10^{51}$ ergs) for $N \sim 10^{11}$. Whether such initial conditions (of very uniformly distributed dark matter "particles") could possibly be produced in an astrophysical context and thus give rise to such purely gravitational "explosions", with observational traces, is beyond the scope of our study. In the context of cosmology we note that the results we have found may be relevant, for example, in theories of structure formation in "hot" or "warm" dark matter cosmologies. In these cases the initial spectrum of density fluctuations is cut-off abruptly below some cosmological scale, and the first structures should form at such very large scales, without prior formation of structures at smaller scales. In this context the physical effects we have observed might then be expected to come into play, leading potentially also to implications for the numerical resolution provided by an N-body discretisation.

Finally let us remark that rather than considering different non-uniform and/or non-spherical initial conditions, the next natural step in this study is to consider the effects of the presence of initial velocity dispersion. While we would expect such dispersion to regulate the collapse and bound above the ejected mass, it would be interesting to see the full dependence of these quantities on N and the amplitude of this velocity dispersion. It would be interesting to focus on a simple class of initial conditions for the velocities, e.g., "waterbag" distributions, studying very carefully the convergence of results for the virialized state as a function of N, and to characterize carefully also the velocity distributions in the virialized states (which we have not discussed here). With respect to predictions of theoretical models such as that of Lynden-Bell (1967), it would be interesting to explore whether by appropriately modifying the energy/mass constraints on the final state better agreement may be obtained than has been observed without such considerations (see, e.g., Arad & Johansson (2005); Levin et al. (2008)).

We thank the Centro E. Fermi (Rome) for the use of computing resources. MJ thanks Steen Hansen for useful discussions, and the Istituto dei Sistemi Complessi, CNR, Rome, for hospitality during several visits.

REFERENCES

Aarseth S., Lin D., Papaloizou J., 1988, Astrophys. J., 324, 288

Aarseth S. J., 2003, Gravitational N-Body Simulations: Tools and Algorithms. Cambridge

Aarseth S., 1974, Astron. Astrophys., 35, 237

Aguilar L., Merritt D., 1990, Astrophys. J., 354, 73

Arad I., Johansson P., 2005, Mon. Not. R. Astron. Soc., 362, 252

Arad I., Lynden-Bell D., 2005, Mon. Not. R. Astron. Soc., 361, 385

Binney J., Tremaine S., 1994, Galactic Dynamics. Princeton University Press

Boily C., Athanassoula E., 2006, Mon. Not. R. Astr. Soc., 369, 608

Boily C., Athanassoula E., Kroupa P., 2002, Mon. Not. R. Astr. Soc., 332, 971

Braun W., Hepp K., 1977, Comm. Math. Phys., 56, 101

Buchert T., Dominguez A., 2005, Astron. Astrophys., 438, 443
Cooray A., Sheth R., 2002, Phys. Rep., 379, 1
David M., Theuns T., 1989, Mon. Not. R. Astr. Soc., 240, 957
Gabrielli A., Joyce M., 2008, Phys. Rev., E77, 031139
Gabrielli A., Sylos Labini F., Joyce M., Pietronero L., 2004, Statistical Physics for Cosmic Structures. Springer
Hansen S., Agertz O., Joyce M., Stadel J., Moore B., Potter D., 2007, Astrophys.J., 656, 631
Hénon M., 1964, Ann. Astrophys., 27, 1
Iguchi O., Sota Y., Nakamichi A., Morikawa M., 2006, Phys.Rev., E73, 046112
Iguchi O., Sota Y., Tatekawa T., Nakamichi A., Morikawa M., 2005, Phys.Rev., E71, 016102
Levin Y., Pakter R., Rizzato F., 2008, Phys. Rev., E78, 021130
Lynden-Bell D., 1967, Mon. Not. R. Astr. Soc., 167, 101
Lynden-Bell D., Wood 1968, Mon. Not. R. Astr. Soc., 138, 496
McGlynn T., 1984, Astrophys. J., 281, 13
Merrall T., Henriksen R., 2003, Astrophys. J., 595, 43
Navarro J. F., Frenk C. S., White S. D. M., 1996, Astrophys. J., 462, 563
Navarro J. F., Frenk C. S., White S. D. M., 1997, Astrophys. J., 490, 493
Padmanabhan T., 1990, Phys. Rept., 188, 285
Peebles P. J. E., 1980, The Large-Scale Structure of the Universe. Princeton University Press
Roy F., Perez J., 2004, Mon. Not. R. Astr. Soc., 348, 62
Springel V., 2005, Mon. Not. R. Ast. Soc., 364, 1105
Springel V., Yoshida N., White S. D. M., 2001, New Astronomy, 6, 79
Theis C., Spurzem R., 1999, Astron. Astrophys., 341, 361
Theuns T., David M., 1990, Astrophys. Sp. Sci., 170, 276
van Albada T., 1982, Mon. Not. R. Astr. Soc., 201, 939
Villumsen J., 1984, Astrophys. J., 284, 75
`www.mpa-garching.mpg.de/gadget/right.html`, 2000

APPENDIX A: GROWTH OF LINEARIZED PERTURBATIONS

After some simple algebra, Eq. (7) reduces to

$$2\frac{d^2\delta}{dR^2}\left(\frac{1}{R}-1\right)+\frac{d\delta}{dR}\left(\frac{3}{R^2}-\frac{4}{R}\right)-\frac{3}{R^3}\delta=0, \qquad \text{(A1)}$$

where we have taken $R(t=0)=1$. The general solution can be written as

$$\delta(R)=A_1\frac{\sqrt{R-1}}{R^{3/2}}+ \qquad \text{(A2)}$$
$$A_2\frac{1}{R^{3/2}}\left(\sqrt{R}(R-3)+3\sqrt{R-1}\ \mathrm{asinh}(\sqrt{R-1})\right)$$

Using the appropriate initial conditions for our case,

$$\delta(R=1)=\delta_0\ , \qquad \frac{d\delta}{dR}(R=1)=\frac{\dot\delta(t=0)}{\dot R(t=0)}=0\ ,$$

it follows that

$$A_1=0\ \ , A_2=-\delta_0/2\ ,$$

and thus $\delta(R)=f(R)\delta_0$ where

$$f(R)=-\frac{1}{2R^{3/2}}\left[\sqrt{R}(R-3)-3\sqrt{1-R}\ \mathrm{asin}(\sqrt{1-R})\right]\ . \qquad \text{(A3)}$$

The behaviour of Eq. (A3) as $R\to 0$, i.e., close to the collapse time, is

$$f(R)=\frac{3\pi}{4}R^{-3/2}+\mathcal{O}(R^{-1/2})\ . \qquad \text{(A4)}$$